# An introduction to orthogonal frequency-division multiplexing

Ove Edfors     Magnus Sandell     Jan-Jaap van de Beek

Daniel Landström     Frank Sjöberg

September 1996

**Abstract**

This report is an introduction to *orthogonal frequency-division multiplexing* (OFDM). The focus is on signal processing areas pursued by our research group at Luleå University of Technology. We present an historical background and some frequently used system models. Typical areas of applications are also described, both wireless and wired. In addition to the general overview, the addressed areas include synchronization, channel estimation and channel coding. Both time and frequency synchronization are described, and the effects of synchronization errors are presented. Different types of channel estimators are described, where the focus is on low-complexity algorithms, and in this context, advantages and disadvantages of coherent and differential modulation are also discussed. Channel coding is described, both for wireless and wired systems, and pointers are included to evaluation tools and bitloading algorithms. An extensive bibliography is also included.

# Contents

# List of Figures

# Chapter 1

# Introduction

The aim of this report is twofold. The first aim is to provide an introduction to *orthogonal frequency-division multiplexing* (OFDM) systems and selected parts of its theoretical background. The second aim is to describe the areas of research within OFDM that are pursued at the Division of Signal Processing, Luleå University. This also includes a (by no means complete) description of related work that may be of interest. The presentation is in the form of a single body, where we do not separate our own work from that by others.

The technology we call OFDM in this report is usually viewed as a collection of transmission techniques. When applied in a wireless environment, such as radio broadcasting, it is usually referred to as OFDM. However, in a wired environment, such as in *asymmetric digital subscriber-lines* (ADSL), the term *discrete multitone* (DMT) is more appropriate. Throughout this report we only use the term DMT when explicitly addressing the wired environment. Further, the two terms *subcarrier* and *subchannel* will be used interchangeably. The history of OFDM has been addressed several times in the literature, see *e.g.* [13, 126], which we have condensed to the brief overview below.

The history of OFDM dates back to the mid 60's, when Chang published his paper on the synthesis of bandlimited signals for multichannel transmission [18]. He presents a principle for transmitting messages simultaneously through a linear bandlimited channel without *interchannel* (ICI) and *intersymbol interference* (ISI). Shortly after Chang presented his paper, Saltzberg performed an analysis of the performance [91], where he concluded that "the strategy of designing an efficient parallel system should concentrate more on reducing crosstalk between adjacent channels than on perfecting the individual channels themselves, since the distortions due to crosstalk tend to dominate". This is an important conclusion, which has proven correct in the digital baseband processing that emerged a few years later.

A major contribution to OFDM was presented in 1971 by Weinstein and Ebert [116], who used the *discrete Fourier transform* (DFT) to perform baseband modulation and demodulation. This work did not focus on "perfecting the individual channels", but rather on introducing efficient processing, eliminating the banks of subcarrier oscillators. To combat ISI and ICI they used both a guard space between the symbols and raised-cosine windowing in the time domain. Their system did not obtain perfect orthogonality between subcarriers over a dispersive channel, but it was still a major contribution to OFDM.

Another important contribution was due to Peled and Ruiz in 1980 [79], who introduced the *cyclic prefix* (CP) or cyclic extension, solving the orthogonality problem. Instead of using an empty guard space, they filled the guard space with a cyclic extension of the OFDM symbol.

1

This effectively simulates a channel performing cyclic convolution, which implies orthogonality over dispersive channels when the CP is longer than the impulse response of the channel. This introduces an energy loss proportional to the length of the CP, but the zero ICI generally motivates the loss.

OFDM systems are usually designed with rectangular pulses, but recently there has been an increased interest in pulse shaping [51, 68, 108]. By using pulses other than rectangular, the spectrum can be shaped to be more well-localized in frequency, which is beneficial from an interference point of view.

OFDM is currently used in the European *digital audio broadcasting* (DAB) standard [1]. Several DAB systems proposed for North America are also based on OFDM [66], and its applicability to digital TV broadcasting is currently being investigated [2, 30, 70, 72, 106]. OFDM in combination with multiple-access techniques are subject to significant investigation, see *e.g.,* [7, 8, 44, 88, 113]. OFDM, under the name DMT, has also attracted a great deal of attention as an efficient technology for high-speed transmission on the existing telephone network, see *e.g.,* [13, 21, 107, 121].

This report is organized as follows: In Section 2 we present common OFDM models, including continuous-time and discrete-time. Environments in which OFDM systems are expected to work are summarized in Section 3. Synchronization problems and proposed solution are presented in Section 4. Channel estimation is elaborated on in Section 5 and coding, in both wireless and wired OFDM systems, is discussed in Section 6. Finally, in Section 7 we discuss and summarize the contents of this report.

# Chapter 2

# System models

The basic idea of OFDM is to divide the available spectrum into several subchannels (subcarriers). By making all subchannels narrowband, they experience almost flat fading, which makes equalization very simple. To obtain a high spectral efficiency the frequency response of the subchannels are overlapping and orthogonal, hence the name OFDM. This orthogonality can be completely maintained, even though the signal passes through a time-dispersive channel, by introducing a cyclic prefix. There are several versions of OFDM, see *e.g.*, [13, 68, 116], but we focus on systems using such a cyclic prefix [79]. A cyclic prefix is a copy of the last part of the OFDM symbol which is prepended to the transmitted symbol, see Figure 2.1. This makes the
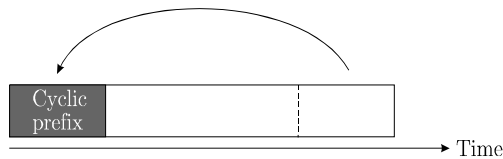


Figure 2.1: The cyclic prefix is a copy of the last part of the OFDM symbol.

transmitted signal periodic, which plays a decisive roll in avoiding intersymbol and intercarrier interference [13]. This is explained later in this section. Although the cyclic prefix introduces a loss in *signal-to-noise ratio* (SNR), it is usually a small price to pay to mitigate interference.

A schematic diagram of a baseband OFDM system is shown in Figure 2.2.
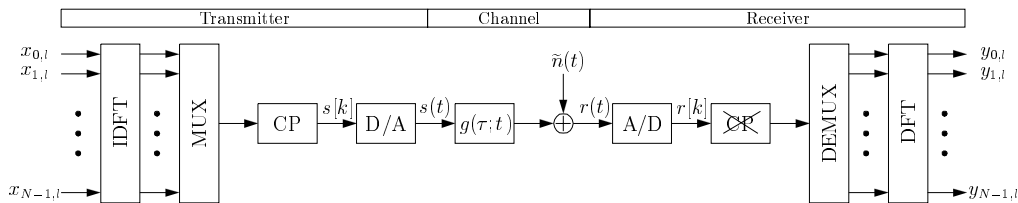


Figure 2.2: A digital implementation of a baseband OFDM system. 'CP' and '⊘P' denote the insertion and deletion of the cyclic prefix, respectively.

For this system we employ the following assumptions:

- A cyclic prefix is used.

- The impulse response of the channel is shorter than the cyclic prefix.

- Transmitter and receiver are perfectly synchronized.

- Channel noise is additive, white, and complex Gaussian.

- The fading is slow enough for the channel to be considered constant during one OFDM symbol interval.

The difficulties in a complete analysis of this system make it rather awkward for theoretical studies. Therefore, it is common practice to use simplified models resulting in a tractable analysis. We classify these OFDM system models into two different classes: continuous-time and discrete-time.

## 2.1 Continuous-time model

The first OFDM systems did not employ digital modulation and demodulation. Hence, the continuous-time OFDM model presented below can be considered as the ideal OFDM system, which in practice is digitally synthesized. Since this is the first model described, we move through it in a step-by-step fashion. We start with the waveforms used in the transmitter and proceed all the way to the receiver. The baseband model is shown in Figure 2.3.
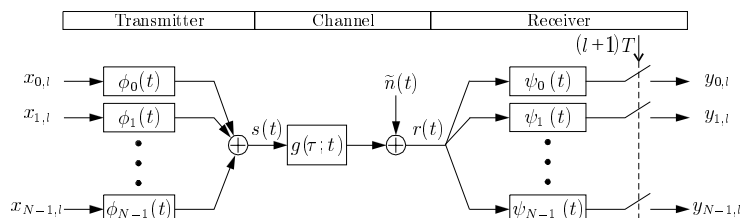


Figure 2.3: Base-band OFDM system model.

- **Transmitter**
  Assuming an OFDM system with $N$ subcarriers, a bandwidth of $W$ Hz and symbol length of $T$ seconds, of which $T_{cp}$ seconds is the length of the cyclic prefix, the transmitter uses the following waveforms

$$\phi_k(t) = \begin{cases} \frac{1}{\sqrt{T-T_{cp}}} e^{j2\pi \frac{W}{N}k(t-T_{cp})} & \text{if } t \in [0,T] \\ 0 & \text{otherwise} \end{cases}, \tag{2.1}$$

where $T = N/W + T_{cp}$. Note that $\phi_k(t) = \phi_k(t + N/W)$ when $t$ is within the cyclic prefix $[0, T_{cp}]$. Since $\phi_k(t)$ is a rectangular pulse modulated on the carrier frequency $kW/N$, the common interpretation of OFDM is that it uses $N$ subcarriers, each carrying a low

4

bit-rate. The waveforms $\phi_k(t)$ are used in the modulation and the transmitted base band signal for OFDM symbol number $l$ is

$$s_l(t) = \sum_{k=0}^{N-1} x_{k,l}\phi_k(t - lT),$$

where $x_{0,l}$, $x_{1,l}$, ..., $x_{N-1,l}$ are complex numbers from a set of signal constellation points. When an infinite sequence of OFDM symbols is transmitted, the output from the transmitter is a juxtaposition of individual OFDM symbols:

$$s(t) = \sum_{l=-\infty}^{\infty} s_l(t) = \sum_{l=-\infty}^{\infty}\sum_{k=0}^{N-1} x_{k,l}\phi_k(t - lT). \tag{2.2}$$

- **Physical channel**
  We assume that the support of the (possibly time variant) impulse response $g(\tau; t)$ of the physical channel is restricted to the interval $\tau \in [0, T_{cp}]$, *i.e.*, to the length of the cyclic prefix. The received signal becomes

$$r(t) = (g * s)(t) = \int_0^{T_{cp}} g(\tau; t)s(t - \tau)d\tau + \widetilde{n}(t), \tag{2.3}$$

where $\widetilde{n}(t)$ is additive, white, and complex Gaussian channel noise.

- **Receiver**
  The OFDM receiver consists of a filter bank, matched to the last part $[T_{cp}, T]$ of the transmitter waveforms $\phi_k(t)$, *i.e.*,

$$\psi_k(t) = \begin{cases} \phi_k^*(T - t) & \text{if } t \in [0, T - T_{cp}] \\ 0 & \text{otherwise} \end{cases}. \tag{2.4}$$

Effectively this means that the cyclic prefix is removed in the receiver. Since the cyclic prefix contains all ISI from the previous symbol, the sampled output from the receiver filter bank contains no ISI. Hence we can ignore the time index $l$ when calculating the sampled output at the $k$th matched filter. By using (2.2), (2.3) and (2.4), we get

$$
\begin{aligned}
y_k &= (r * \psi_k)(t)|_{t=T} = \int_{-\infty}^{\infty} r(t)\psi_k(T - t)\,dt \\
&= \int_{T_{cp}}^{T}\left(\int_0^{T_{cp}} g(\tau; t)\left[\sum_{k'=0}^{N-1} x_{k'}\phi_{k'}(t - \tau)\right]d\tau\right)\phi_k^*(t)\,dt + \int_{T_{cp}}^{T}\widetilde{n}(T - t)\phi_k^*(t)\,dt.
\end{aligned}
$$

We consider the channel to be fixed over the OFDM symbol interval and denote it by $g(\tau)$, which gives

$$y_k = \sum_{k'=0}^{N-1} x_{k'}\int_{T_{cp}}^{T}\left(\int_0^{T_{cp}} g(\tau)\phi_{k'}(t - \tau)d\tau\right)\phi_k^*(t)\,dt + \int_{T_{cp}}^{T}\widetilde{n}(T - t)\phi_k^*(t)\,dt.$$

5

The integration intervals are $T_{cp} < t < T$ and $0 < \tau < T_{cp}$ which implies that $0 < t - \tau < T$ and the inner integral can be written as

$$
\begin{aligned}
\int_0^{T_{cp}} g(\tau)\phi_{k'}(t-\tau)d\tau &= \int_0^{T_{cp}} g(\tau)\frac{e^{j2\pi k'(t-\tau-T_{cp})W/N}}{\sqrt{T-T_{cp}}}d\tau \\
&= \frac{e^{j2\pi k'(t-T_{cp})W/N}}{\sqrt{T-T_{cp}}}\int_0^{T_{cp}} g(\tau)e^{-j2\pi k'\tau W/N}d\tau, \quad T_{cp} < t < T
\end{aligned}
$$

The latter part of this expression is the sampled frequency response of the channel at frequency $f = k'W/N$, i.e., at the $k'$th subcarrier frequency:

$$
h_{k'} = G\left(k'\frac{W}{N}\right) = \int_0^{T_{cp}} g(\tau)e^{-j2\pi k'\tau W/N}d\tau, \tag{2.5}
$$

where $G(f)$ is the Fourier transform of $g(\tau)$. Using this notation the output from the receiver filter bank can be simplified to

$$
\begin{aligned}
y_k &= \sum_{k'=0}^{N-1} x_{k'}\int_{T_{cp}}^{T} \frac{e^{j2\pi k'(t-T_{cp})W/N}}{\sqrt{T-T_{cp}}}h_{k'}\phi_k^*(t)\,dt + \int_{T_{cp}}^{T} \widetilde{n}(T-t)\phi_k^*(t)\,dt \\
&= \sum_{k'=0}^{N-1} x_{k'}h_{k'}\int_{T_{cp}}^{T}\phi_{k'}(t)\phi_k^*(t)\,dt + n_k, \tag{2.6}
\end{aligned}
$$

where $n_k = \int_{T_{cp}}^{T}\widetilde{n}(T-t)\phi_k^*(t)\,dt$. Since the transmitter filters $\phi_k(t)$ are orthogonal,

$$
\int_{T_{cp}}^{T}\phi_{k'}(t)\phi_k^*(t)\,dt = \int_{T_{cp}}^{T}\frac{e^{j2\pi k'(t-T_{cp})W/N}}{\sqrt{T-T_{cp}}}\frac{e^{-j2\pi k(t-T_{cp})W/N}}{\sqrt{T-T_{cp}}}dt = \delta[k-k'],
$$

where $\delta[k]$ is the Kronecker delta function [78], we can simplify (2.6) and obtain

$$
y_k = h_k x_k + n_k, \tag{2.7}
$$

where $n_k$ is *additive white Gaussian noise* (AWGN).

The benefit of a cyclic prefix is twofold: it avoids both ISI (since it acts as a guard space) and ICI (since it maintains the orthogonality of the subcarriers). By re-introducing the time index $l$, we may now view the OFDM system as a set of parallel Gaussian channels, according to Figure 2.4.

An effect to consider at this stage is that the transmitted energy increases with the length of the cyclic prefix, while the expressions for the received and sampled signals (2.7) stay the same. The transmitted energy per subcarrier is $\int |\phi_k(t)|^2\,dt = T/(T-T_{cp})$, and the SNR loss, because of the discarded cyclic prefix in the receiver, becomes

$$
\text{SNR}_{loss} = -10\log_{10}(1-\gamma),
$$

where $\gamma = T_{cp}/T$ is the relative length of the cyclic prefix. The longer the cyclic prefix, the larger the SNR loss. Typically, the relative length of the cyclic prefix is small and the ICI- and ISI-free transmission motivates the SNR loss (less than 1 dB for $\gamma < 0.2$).
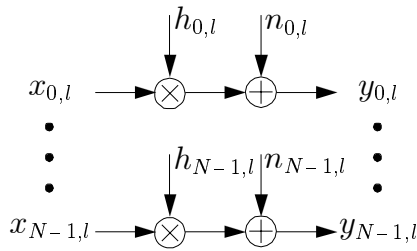
Figure 2.4: The continuous-time OFDM system interpreted as parallel Gaussian channels.
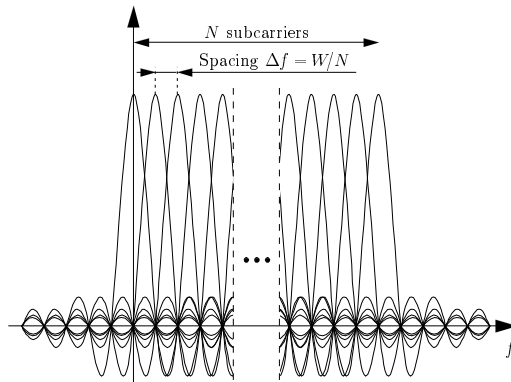


Figure 2.5: A symbolic picture of the individual subchannels for an OFDM system with $N$ tones over a bandwidth $W$.

Figure 2.5 displays a schematic picture of the frequency response of the individual subchannels in an OFDM symbol. In this figure the individual subchannels of the system are separated. The rectangular windowing of the transmitted pulses results in a sinc-shaped frequency response for each channel. Thus, the power spectrum of the OFDM system decays as $f^{-2}$. In some cases this is not sufficient and methods have been proposed to shape the spectrum. In [116], a raised cosine-pulse is used where the roll-off region also acts as a guard space, see Figure 2.6. If the flat part is the OFDM symbol, including the cyclic prefix, both
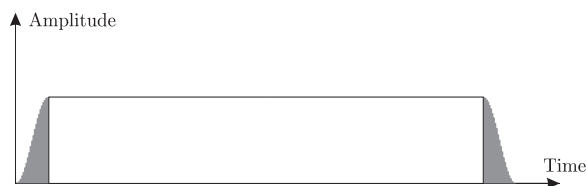


Figure 2.6: Pulse shaping using the raised-cosine function. The gray parts of the signal indicate the extensions.

ICI and ISI are avoided. The spectrum with this kind of pulse shaping is shown in Figure 2.7, where it is compared with a rectangular pulse. The overhead introduced by an extra guard space with a graceful roll-off can be a good investment, since the spectrum falls much more quickly and reduces the interference to adjacent frequency bands.
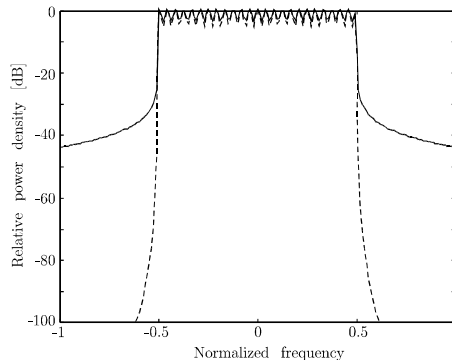
Figure 2.7: Spectrum with rectangular pulse (solid) and raised-cosine pulse (dashed).

Other types of pulse shaping, such as overlapping [108] and well localized pulses [51, 68], have also been investigated.

## 2.2  Discrete-time model

An entirely discrete-time model of an OFDM system is displayed in Figure 2.8. Compared to the continuous-time model, the modulation and demodulation are replaced by an *inverse DFT* (IDFT) and a DFT, respectively, and the channel is a discrete-time convolution. The cyclic prefix operates in the same fashion in this system and the calculations can be performed in essentially the same way. The main difference is that all integrals are replaced by sums.
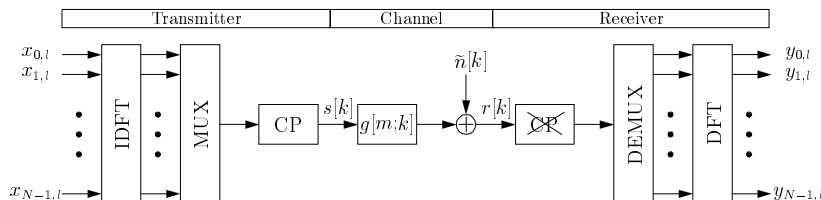


Figure 2.8: Discrete-time OFDM system.

From the receiver's point of view, the use of a cyclic prefix longer than the channel will transform the linear convolution in the channel to a cyclic convolution. Denoting cyclic convolution by '⊛', we can write the whole OFDM system as

$$\begin{aligned} \mathbf{y}_l &= \mathrm{DFT}\left(\mathrm{IDFT}\left(\mathbf{x}_l\right) \circledast \mathbf{g}_l + \widetilde{\mathbf{n}}_l\right) \\ &= \mathrm{DFT}\left(\mathrm{IDFT}\left(\mathbf{x}_l\right) \circledast \mathbf{g}_l\right) + \mathbf{n}_l, \end{aligned}$$

where $\mathbf{y}_l$ contains the $N$ received data points, $\mathbf{x}_l$ the $N$ transmitted constellation points, $\mathbf{g}$ the channel impulse response of the channel (padded with zeros to obtain a length of $N$), and $\widetilde{\mathbf{n}}_l$ the channel noise. Since the channel noise is assumed white and Gaussian, the term $\mathbf{n}_l = \mathrm{DFT}\left(\widetilde{\mathbf{n}}_l\right)$ represents uncorrelated Gaussian noise. Further, we use that the DFT of two cyclically convolved signals is equivalent to the product of their individual DFTs. Denoting

8

element-by-element multiplication by '·', the above expression can be written

$$\mathbf{y}_l = \mathbf{x}_l \cdot \mathrm{DFT}\,(\mathbf{g}_l) + \mathbf{n}_l = \mathbf{x}_l \cdot \mathbf{h}_l + \mathbf{n}_l,$$

where $\mathbf{h}_l = \mathrm{DFT}\,(\mathbf{g}_l)$ is the frequency response of the channel. Thus we have obtained the same type of parallel Gaussian channels as for the continuous-time model. The only difference is that the channel attenuations $\mathbf{h}_l$ are given by the $N$-point DFT of the discrete-time channel, instead of the sampled frequency response as in (2.5).

## 2.3   A time-frequency interpretation

The models described above are two classical models of OFDM with a cyclic prefix. A more general model, suitable for *e.g.*, pulse shaping, is to view OFDM as transmission of data in a lattice in the time-frequency plane. Consider first a transmitted OFDM signal $s(t)$

$$s(t) = \sum_{k,l} x_{k,l}\phi_{k,l}(t),$$

where the functions $\phi_{k,l}(t)$ are translations in time by $\tau_0$ and in frequency by $\nu_0$ of the prototype function $p(t)$, *i.e.*,

$$\phi_{k,l}(t) = p\,(t - l\tau_0)\,e^{j2\pi k\nu_0 t}.$$

This creates a *two-dimensional* (2-D) lattice in the time-frequency plane [51, 68], see Figure 2.9. Usually the prototype function is chosen as the rectangular window $p(t) = \frac{1}{\sqrt{\tau_0}}$, $0 \le t \le \tau_0$.
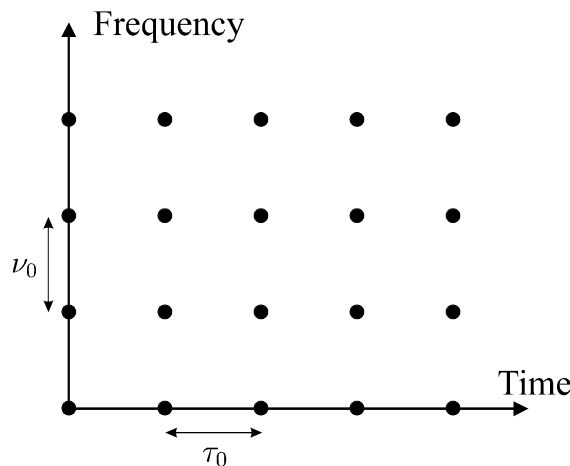


Figure 2.9: Lattice in the time-frequency plane. The data symbols $x_{k,l}$ are transmitted at the lattice points.

The spacing in the frequency direction is then $\nu_0 = 1/\left(\tau_0 - T_{cp}\right)$, where $T_{cp}$ is the length of the cyclic prefix. For a discussion on the impact of prototype functions, see Appendix A. Each transmitted data symbol in the lattice experiences flat fading, see (2.7), which simplifies equalization and channel estimation. The channel attenuations at the lattice points are correlated and by transmitting known symbols at some postions, the channel attenuations can be

estimated with an interpolation filter [51, 56, 92]. This is a 2-D version of pilot-symbol assisted modulation, which has been proposed for several wireless OFDM systems, see *e.g.*, [2, 7, 56]. A more detailed description of OFDM channel estimation is given in Section 5.

## 2.4   Imperfections

Depending on the analyzed situation, imperfections in a real OFDM system may be ignored or explicitly included in the model. Below we mention some of the imperfections and their corresponding effects.

- **Dispersion**

  Both time and frequency dispersion of the channel can destroy the orthogonality of the system, *i.e.*, introduce both ISI and ICI [68]. If these effects are not sufficiently mitigated by *e.g.*, a cyclic prefix and a large inter-carrier spacing, they have to be included in the model. One way of modelling these effects is an increase of the additive noise [75].

- **Nonlinearities and clipping distortion**

  OFDM systems have high peak-to-average power ratios and high demands on linear amplifiers [96]. Nonlinearities in amplifiers may cause both ISI and ICI in the system. Especially, if the amplifiers are not designed with proper *output back-off* (OBO), the clipping distortion may cause severe degradation. These effects have been addressed in *e.g.*, [20, 31, 49, 86]. Special coding strategies with the aim to minimize peak-to-average power ratios have also been suggested, see *e.g.,* [61, 62, 76].

- **External interference**

  Both wireless and wired OFDM systems suffer from external interference. In wireless systems this interference usually stems from radio transmitters and other types electronic equipment in the vincinity of the receiver. In wired systems the limiting factor is usually crosstalk, which is discussed in more detail in Section 3.2.2. Interference can be included in the model as *e.g.*, colored noise.

# Chapter 3

# System environments

Two major groups of communication systems are those who operate in wireless and wired environments. For instance, when designing a wireless OFDM system the fading channel is usually a major obstacle, while for a wired OFDM (*a.k.a.* DMT) system crosstalk and impulsive noise are more difficult to handle.

In the following sections we briefly discuss the wireless and wired environments.

## 3.1   Wireless systems

In wireless systems (radio systems), changes in the physical environment cause the channel to fade. These changes include both relative movement between transmitter and receiver and moving scatterers/reflectors in the surrounding space.

When developing new standards for wireless systems, channel models are usually classified according to the environment in which the receiver operates. These environments are often described in terms like "Rural area", "Business indoor", etc. Models of this type are specified by *e.g.*, the *European telecommunications standards institute* (ETSI) [3, 4].

In theoretical studies of wireless systems, the channel models are usually chosen so that they result in a tractable analysis. The two major classes of fading characteristics are known as Rayleigh and Rician [83]. A Rayleigh-fading environment assumes no line-of-sight and no fixed reflectors/scatterers. The expected value of the fading is zero. If there is a line-of-sight, this can be modelled by Rician-fading, which has the same characteristics as the Rayleigh-fading, except for a non-zero expected value.

Often properties of a theoretical model are characterized by only a few parameters, such as power-delay profile and maximal Doppler frequency. The power-delay profile $\rho(\cdot)$ depends on the environment and a common choice is the exponentially decaying profile

$$\rho(\tau) = e^{-\tau/\tau_{rms}},$$

where $\tau$ is the time delay and $\tau_{rms}$ is the *root mean-squared* (RMS) value of the power-delay profile. Several other choices are possible, see *e.g.,* [57]. The maximal Doppler frequency $f_{d,\max}$ can be determined by

$$f_{d,\max} = f_c \frac{v}{c},$$

where the carrier frequency is $f_c$ Hz, the speed of the receiver is $v$ m/s, and the speed of light is $c \approx 3 \times 10^8$ m/s. Isotropic scattering is commonly assumed, *i.e.* the received signal power

is spread uniformly over all angles of arrival, which results in a U-shaped Doppler spectrum. This is usually referred to as a Jakes spectrum [59], and is determined by the maximal Doppler frequency.

Before we start discussing the different scenarios encountered in wireless systems, there are a few things that may be said about OFDM on fading channels in general:

1. The inter-carrier spacing of the system has to be chosen large, compared to the maximal Doppler frequency of the fading channel, to keep the ICI small [75, 89]. This is further discussed in Appendix A.

2. If the orthogonality of the system is maintained, the basic OFDM structure does not necessitate traditional equalizing. However, to exploit the diversity of the channel, proper coding and interleaving is required [118].

We have chosen to discuss the wireless environment in two contexts: the transmission from a base-station to mobile terminals (downlink) and the transmission from mobile terminals to a base-station (uplink). The reason for the chosen contexts is that one or both usually are represented in every wireless system, and they require quite different design strategies.

The most frequently discussed wireless OFDM systems are for broadcasting, *e.g.,* digital audio and digital video, and only contain a downlink, since there is no return channel. Cellular systems, on the other hand, have both a downlink and an uplink.

### 3.1.1   Downlink

A schematic picture of the downlink environment is shown in Figure 3.1. In this case, mobile terminal number $n$ receives the signal $s(t)$ transmitted from the base station through its own channel $g_n(t)$, and the received signal $r_n(t)$ is given by

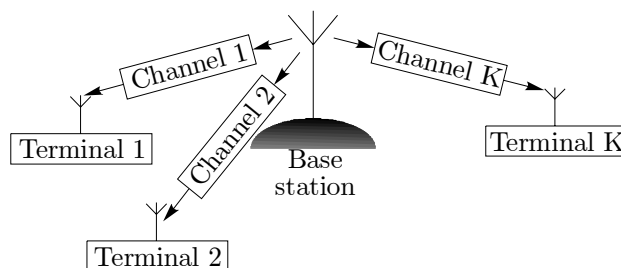$$r_n(t) = (s * g_n)(t).$$



Figure 3.1: The wireless downlink environment.

This environment implies that each receiver (terminal) only has to synchronize to the base station and, from its point of view, the other terminals do not exist. This makes synchronization relatively easy and all pilot information transmitted from the base station can be used for channel estimation and synchronization.

The downlink environment has been thoroughly investigated (see *e.g.,* [5, 24, 44, 87, 88]). Large portions of work presented on systems of this kind have been concerned with digital audio (see *e.g.,* [1, 5, 56, 69, 118]) and digital video (see *e.g.,* [2, 30, 90, 95, 106, 120, 126]) broadcasting.

### 3.1.2 Uplink

A schematic picture of the uplink environment is shown in Figure 3.2. In this case, the base station receives the transmitted signal $s_n(t)$ from mobile terminal $n$ through channel $g_n(t)$, and the total received signal $r(t)$ at the base station is a superposition

$$r(t) = \sum_{n=1}^{K} (s_n * g_n)(t)$$
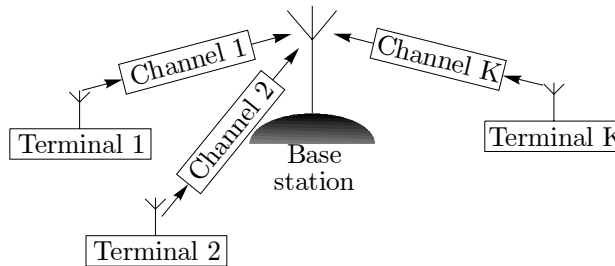
of signals from all mobile terminals.



Figure 3.2: The wireless uplink environment.

The major problem here is the superposition of signals arriving through different channels. For the base station to be able to separate the signals from each receiver, a sufficient orthogonality between received signals, from different terminals, has to be achieved. Several methods for obtaining this have been proposed. These include combinations of OFDM and *code-division*, *time-division* and *frequency-division multiple access* (CDMA, TDMA and FDMA, respectively). All three have been proposed in [88] and FDMA/OFDM is currently under investigation in *e.g.,* [7, 8, 113].

Independent of the method chosen to separate signals from different terminals, the system synchronization is one of the major design issues. To avoid interference all mobile terminals have to be jointly synchronized to the base station. Further, if coherent modulation is used, as in [7, 8, 113], the different channels from the users have to be estimated separately.

## 3.2 Wired systems

When studying wired communication systems and transmission characteristics of cables, a distinction is often made between shielded cables (like coaxial cables) and unshielded cables (like twisted wire pairs). Coaxial cables have much better transmission properties for broadband signals than do wire pairs. Except for computer networks, coaxial cables and wire pairs currently exist in two basically different network topologies.

Wire pairs are the dominating cable type in telephone access networks that are built for point to point and two way communication. Coaxial cables are usually found in cable TV systems, a network topology that is primarily intended for broadcasting and not for point to point communication. The cable TV systems sometimes contain amplifiers that make bidirectional communication almost impossible. However, cable TV networks are currently being upgraded to support bidirectional communication. We focus on wire pairs and will not discuss coaxial cables further.

The copper wire pair does not change its physical behavior significantly with time and is therefore considered a stationary channel [117]. This makes it possible to use a technique called bit loading [13] (see Section 6.2.1), which makes good use of the spectrally shaped channel. When bit loading is used in a wired OFDM system, it is often referred to as DMT.

Since OFDM in combination with bit loading makes efficient use of available bandwidth it has become a good candidate for *digital subscriber-line* (DSL) systems. DSL is another name for digital high speed communication in the telephone access network.

When the bit rate offered in downstream direction (to the subscriber) is larger than the bit rate in upstream direction (to the base), it is called an *asymmetric digital subscriber-line* (ADSL). ADSL is suitable for applications like video on demand, games, virtual shopping, internet surfing etc., where most of the data goes from the base to the subscriber. In the USA there exists an ADSL standard that supports downstream bit rates from 1.54 to 6.1 Mbits/s [121]. The bit rates of the upstream return path usually ranges between 9.6 and 192 kbits/s [124].

Standards for symmetrical DSLs have also emerged to support video conferencing and other services with high data rate in the upstream direction. The first symmetric DSL system was called *high bit-rate digital subscriber-line* (HDSL) [22], which currently supports bit rates between 1.5 and 2.1 Mbits/sec in both directions [22, 117]. For digital subscriber lines with higher bit rates than HDSL and ADSL the term *very high bit-rate digital subscriber-line* (VDSL) is used.

### 3.2.1   Subscriber-line transfer function

The characteristics of the wire pair channel have been studied in a number of papers [27, 117, 121]. A thorough description of the transfer function of copper wires and noise sources is given by Werner in [117].

For DSLs using a large frequency range, several MHz or higher, the attenuation function can then be approximated as

$$|H(f,d)|^2 = e^{-dk\sqrt{f}},$$

where $d$ is the length of the cable and $k$ is a cable constant. This model is often used when VDSL and HDSL systems are analyzed [63, 64].

### 3.2.2   Noise and crosstalk

The most important noise sources in the subscriber-line environment are crosstalk from other wire pairs in the same cable, *radio frequency* (RF) noise from nearby radio transmitters, and impulse noise from relays, switches, electrical machines, etc. AWGN is generally not a limiting factor in digital subscriber-lines for short cables, but becomes more important with increasing

cable length. In *e.g.,* [22] AGWN is included in the channel model with a spectral density of $-140$ dBm/Hz, $(1.7\mu V/\sqrt{Hz})$.

Impulse noise is difficult to characterize completely but some efforts has been made to model this kind of disturbances [27, 117]. The normal way to mitigate the effects of impulse noise on a DMT system is to add 6-12 dB to the system margin [23] and to use specially designed codes [21]. It should be noted that DMT is more resistant to impulse noise than single-carrier systems such as *carrierless amplitude/phase* (CAP) modulation [48]. The impact of RF noise on a DSL system can be reduced significantly with OFDM and bit loading [121]. RF noise can be modelled as narrowband disturbance with known spectral density and the *bit-error rate* (BER) can be preserved by transmitting fewer (sometimes zero) bits on the disturbed subchannels.

There are basically two different forms of crosstalk: *near-end crosstalk* (NEXT) and *far-end crosstalk* (FEXT). NEXT occurs at the central office (base station) when the weak upstream signal, $r(t)$, is disturbed by strong downstream signals, $s(t)$, see Figure 3.3. FEXT is crosstalk from one transmitted signal, $s(t)$, to another, $r(t)$, in the same direction, see Figure 3.4, and appears at both ends of the wire loop.
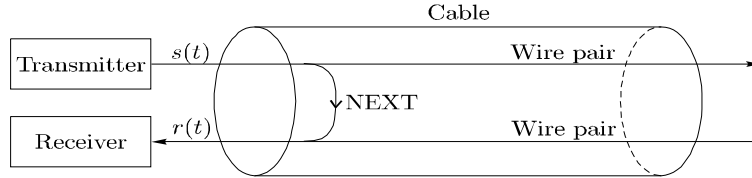


Figure 3.3: Near-end crosstalk (NEXT).
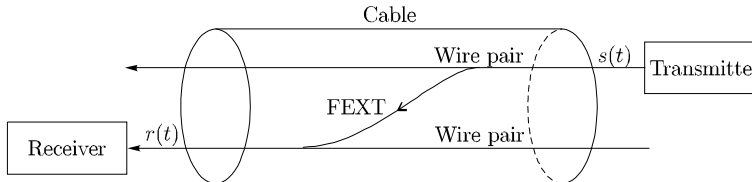


Figure 3.4: Far-end crosstalk (FEXT).

The spectral density of NEXT is modelled in [117] as

$$P_N(f) = P_s(f) k_N f^{3/2}, \tag{3.1}$$

and the spectral density of FEXT as

$$P_F(f,d) = P_s(f) k_F f^2 |H(f,d)|^2 d = P_s(f) k_F f^2 e^{-dk\sqrt{f}} d, \tag{3.2}$$

where $P_s(f)$ is the spectral density of the transmitted signals, $k_N$ and $k_F$ are constants depending on the type of cable, how well balanced the cables are, and the number of disturbing copper pairs [117]. Note that NEXT does not depend on the length of the wire pair.

In Figure 3.5 we display an example of the spectral density of a received signal, NEXT, and FEXT.

Figure 3.5: Power spectral density of attenuated signal, NEXT and FEXT.

# Chapter 4

# Synchronization

One of the arguments against OFDM is that it is highly sensitive to synchronization errors, in particular, to frequency errors [96]. Here we give an overview of three synchronization prob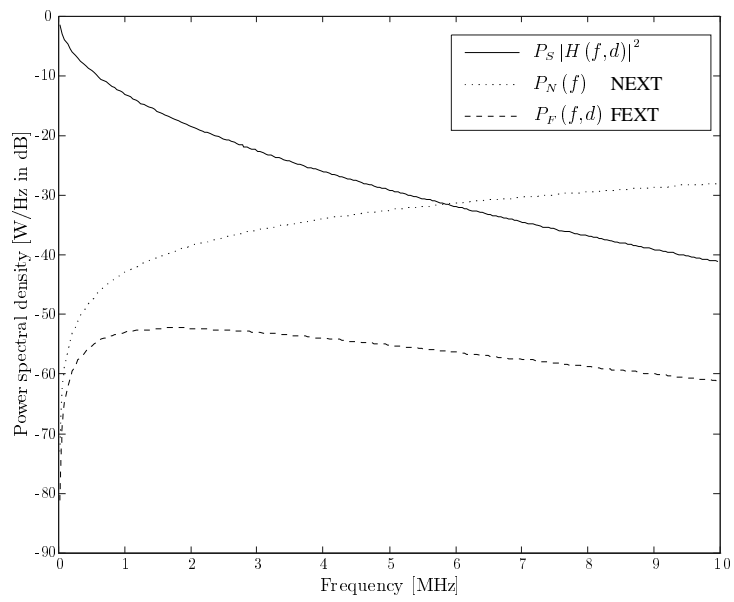lems: symbol, carrier frequency and sampling frequency synchronization. Also, the effects of phase offsets and phase noise are discussed.

## 4.1 Symbol synchronization

### 4.1.1 Timing errors

A great deal of attention is given to symbol synchronization in OFDM systems. However, by using a cyclic prefix, the timing requirements are relaxed somewhat. The objective is to know when the symbol starts. The impact of timing errors has been analyzed in [80, 115]. A timing offset gives rise to a phase rotation of the subcarriers. This phase rotation is largest on the edges of the frequency band. If a timing error is small enough to keep the channel impulse response within the cyclic prefix, the orthogonality is maintained. In this case a symbol timing delay can be viewed as a phase shift introduced by the channel, and the phase rotations can be estimated by a channel estimator. If a time shift is larger than the cyclic prefix, ISI will occur.

There are two main methods for timing synchronization: based on pilots or on the cyclic prefix. An algorithm of the former kind was suggested by Warner and Leung in [114]. They use a scheme where the OFDM signal is transmitted by *frequency modulation* (FM). The transmitter encodes a number of reserved subchannels with known phases and amplitudes. The synchronization technique, with modifications, is applicable to OFDM signals transmitted by amplitude modulation. Their algorithm consists of 3 phases: power detection , coarse synchronization and fine synchronization.

The first phase (power detection) detects whether or not an OFDM signal is present by measuring the received power and compare it to a threshold. The second phase (coarse synchronization) is used to acquire synchronization alignment to within ±0.5 samples. This performance is not acceptable, but this phase serves to simplify the tracking algorithm (which can assume that the timing error is small). The coarse synchronization is done by correlating the received signal to a copy of the transmitted synchronization signal. To find the peak of this correlation with enough accuracy, a digital filter is used to provide interpolated data values

at four times the original data rate. In the last phase (fine synchronization) of the synchronization, the subchannels with pilots are equalized with the estimated channel obtained from pilots. Since the coarse synchronization guarantees that the timing error is less than $\pm 0.5$, the channel impulse response is within the cyclic prefix. The remaining phase errors on the pilot subchannels are due to timing error and can be estimated by linear regression.

There are also synchronization algorithms based on the cyclic prefix. In [106] the difference between received samples spaced $N$ samples apart is formed, $r(k) - r(k + N)$. When one of the samples belongs to the cyclic prefix and the other one to the OFDM symbol from which it is copied, the difference should be small. Otherwise the difference (between two uncorrelated random variables) will have twice the power, and hence, on average, will be larger. By windowing this difference with a rectangular window of the same length as the cyclic prefix, the output signal has a minimum when a new OFDM symbol starts.

This idea is more formally elaborated in [10, 11, 93]. The likelihood function given the observed signal $r(k)$ with a timing and frequency error is derived in [10, 93]. This function is maximized to simultaneously obtain estimates of both timing and frequency offsets. With no frequency offset the likelihood function with respect to a timing offset $\theta$ is

$$\Lambda(\theta) = \sum_{k=\theta}^{\theta+L-1} \frac{2}{\text{SNR}+1} \text{Re}\left\{r(k)r^*(k+N)\right\} - \frac{\text{SNR}}{\text{SNR}+1} |r(k) - r(k+N)|^2$$

For medium and high SNRs (SNR $\gg$ 1) a *maximum likelihood* (ML) estimator based on $\Lambda(\theta)$ essentially applies a moving average to the term $|r(k) - r(k+N)|^2$, *i.e.*, the same as the estimator in [106]. However, for small SNR values the crosscorrelation $r(k)r^*(k+N)$ also has to be taken into account. A similar procedure is used in [11] with the difference that the inphase and quadrature parts of the observed signal $r(k)$ are quantized to 1 bit before $\theta$ is estimated. This yields a symbol synchronizer with a low complexity that can be used in an acquisition mode.

Synchronization in the uplink is more difficult than in the downlink or in broadcasting. This is due to the fact that there will be a separate offset for each user. This problem has not yet been given much attention in the literature. However, a random access sequence is used to synchronize the mobile and the base station in [112]. Interference due to non-synchronized transmission has been investigated in [50].

### 4.1.2 Carrier phase noise

Carrier phase noise is caused by imperfections in the transmitter and receiver oscillators. For a frequency-selective channel, no distinction can be made between the phase rotation introduced by a timing error and a carrier phase offset [80]. An analysis of the impact of carrier phase noise is done in [82]. There it is modelled as a Wiener process $\theta(t)$ with $E\{\theta(t)\} = 0$ and $E\left\{(\theta(t_0 + t) - \theta(t_0))^2\right\} = 4\pi\beta|t|$, where $\beta$ (in Hz) denotes the one-sided 3 dB linewidth of the Lorentzian power density spectrum of the free-running carrier generator. The degradation in SNR, *i.e.*, the increase in SNR needed to compensate for the error, can be approximated by

$$D \text{ (dB)} \approx \frac{11}{6\ln 10}\left(4\pi N \frac{\beta}{W}\right)\frac{E_s}{N_0},$$

where $W$ is the bandwidth and $E_s/N_0$ is the per-symbol SNR. Note that the degradation increases with the number of subcarriers. Due to the rapid variations of the phase noise, it may cause large problems. Analysis of the impact of phase noise in coded systems has been done in [111].

## 4.2 Sampling-frequency synchronization

The received continuous-time signal is sampled at instants determined by the receiver clock. There are two types of methods of dealing with the mismatch in sampling frequency. In synchronized-sampling systems a timing algorithm controls a voltage-controlled crystal oscillator in order to align the receiver clock with the transmitter clock. The other method is non-synchronized sampling where the sampling rate remains fixed, which requires post-processing in the digital domain. The effect of a clock frequency offset is twofold: the useful signal component is rotated and attenuated and, in addition, ICI is introduced. In [81] the bit-error rate performance of a non-synchronized sampled OFDM system has been investigated. It is shown that non-synchronized sampling systems are much more sensitive to a frequency offset, compared with a synchronized-sampling system. For non-synchronized sampling systems, it was shown that the degradation (in dB) due to a frequency sampling offset depends on the square of the carrier index and on the square of the relative frequency offset.

Errors in the sampling frequency for DMT systems have been analyzed in [125].

## 4.3 Carrier frequency synchronization

### 4.3.1 Frequency errors

Frequency offsets are created by differences in oscillators in transmitter and receiver, Doppler shifts, or phase noise introduced by non-linear channels. There are two destructive effects caused by a carrier frequency offset in OFDM systems. One is the reduction of signal amplitude (the sinc functions are shifted and no longer sampled at the peak) and the other is the introduction of ICI from the other carriers, see Figure 4.1. The latter is caused by the loss of orthogonality between the subchannels. In [82], Pollet, *et al.,* analytically evaluate the degradation of the BER caused by the presence of carrier frequency offset and carrier phase noise for an AWGN channel. It is found that a multicarrier system is much more sensitive than a single-carrier system. Denote the relative frequency offset, normalized by the subcarrier spacing, by $\Delta f = \frac{\Delta F}{W/N}$, where $\Delta F$ is the frequency offset and $N$ the number of subcarriers. The degradation $D$ in SNR (in dB) can then be approximated by

$$ D \ (\text{dB}) \approx \frac{10}{3 \ln 10} \left( \pi \Delta f \right)^2 \frac{E_s}{N_0} = \frac{10}{3 \ln 10} \left( \pi \frac{N \cdot \Delta F}{W} \right)^2 \frac{E_s}{N_0}. $$

Note that the degradation (in dB) increases with the square of the number of subcarriers, if $\Delta F$ and $W$ are fixed.

In [74], Moose derives the *signal-to-interference-ratio* (SIR) on a fading and dispersive channel. The SIR is defined as the ratio of the power of the useful signal to the power of the
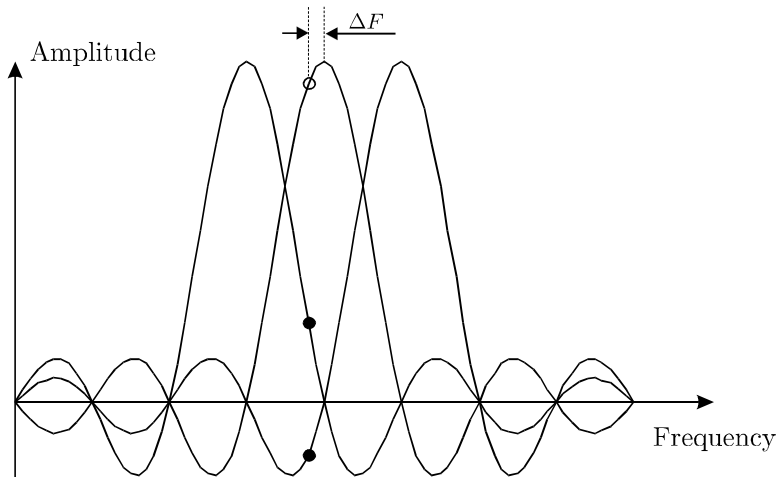
Figure 4.1: Effects of a frequency offset $\Delta F$: reduction in signal amplitude ($\circ$) and intercarrier interference ($\bullet$).

interference signal (ICI and additive noise). He assumed that all channel attenuations $h_k$ have the same power, $E\left\{|h_k|^2\right\}$. An upper bound on the degradation is

$$D \text{ (dB)} \leq 10 \log_{10} \left( \frac{1 + 0.5947 \frac{E_s}{N_0} \sin^2 \pi \Delta f}{\operatorname{sinc}^2 \Delta f} \right), \qquad (4.1)$$

where $\operatorname{sinc} x \triangleq (\sin \pi x) / (\pi x)$. The factor 0.5947 is found from a lower bound of the summation of all interfering subcarriers. In Figure 4.2 the degradation is plotted as a function of the normalized frequency offset $\Delta f$, *i.e.* relative to the subcarrier spacing. The synchronization
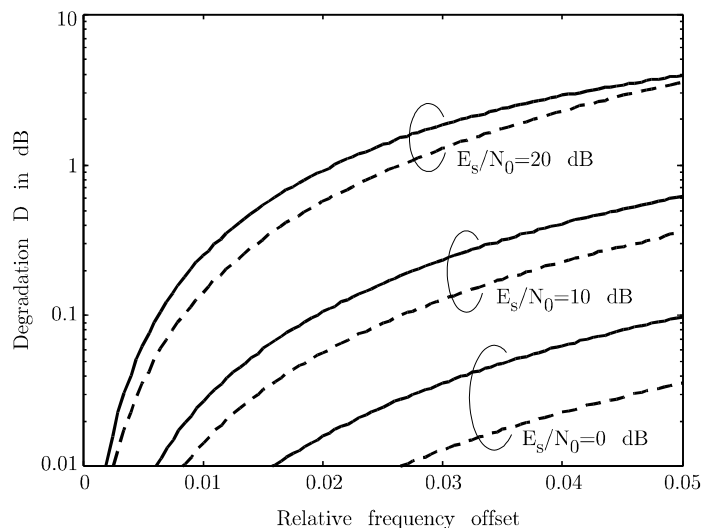


Figure 4.2: Degradation in SNR due to a frequency offset (normalized to the subcarrier spacing). Analytical expression for AWGN (dashed) and fading channels (solid).

requirements for an OFDM system have been investigated in [115]. The conclusion therein is

20

that in order to avoid severe degradation the frequency synchronization accuracy should be better than 2%.

## 4.3.2   Frequency estimators

Several carrier synchronization schemes have been suggested in the literature. As with symbol synchronization, they can be divided into two categories: based on pilots or on the cyclic prefix. Below follows a short overview of some of them.

Pilot-aided algorithms have been addressed in [25]. In that work some subcarriers are used for the transmission of pilots (usually a *pseudo-noise* (PN) sequence). Using these known symbols, the phase rotations caused by the frequency offset can be estimated. Under the assumption that the frequency offset is less than half the subcarrier spacing, there is a one-to-one correspondence between the phase rotations and the frequency offset. To assure this, an acquisition algorithm must be applied. In [25] such an algorithm is constructed by forming a function which is sinc-shaped and has a peak for $f - \widehat{f} = 0$. It was found that by evaluating this function in points $0.1/T$ apart, an acquisition could be obtained by maximizing that function. This acquisition scheme was confirmed by computer simulations to work well both for an AWGN channel and a fading channel.

A related technique is to use the cyclic prefix which, to some extent, can be viewed as pilots. The redundancy of the cyclic prefix can be used in several ways: *e.g.,* by creating a function that peaks at zero offset and finding its maximizing value [28, 106] or by doing maximum likelihood estimation [29, 65, 74, 93]. In [74] it is assumed that the cyclic prefix has the same size as the OFDM symbol (*i.e.* the useful symbol is transmitted twice), in [29] averaging is performed to remove the data dependence and in [65] decision direction is used. In [93] the likelihood function for both timing and frequency offsets is derived by assuming a non-dispersive channel and by considering the transmitted data symbols $x_k$ uncorrelated. By maximizing this function, a simultaneous estimation of the timing and frequency offsets can be obtained. If the frequency error is slowly varying compared the OFDM symbol rate, a *phase-locked loop* (PLL) [83] can be used to reduce the error further.

It is interesting to note the relationship between time and frequency synchronization. If the frequency synchronization is a problem, it can be reduced by lowering the number of subcarriers which will increase the subcarrier spacing. This will, however, increase the demands on the time synchronization, since the symbol length gets shorter, *i.e.* a larger relative timing error will occur. Thus, the synchronizations in time and frequency are closely related to each other.

# Chapter 5

# Channel estimation

Modulation can be classified as differential or coherent. When using differential modulation, there is no need for a channel estimate, since the information is encoded in the difference between two consecutive symbols. This is a common technique in wireless systems, which, since no channel estimator is needed, reduces the complexity of the receiver. Differential modulation is used in the European DAB standard [1]. The drawbacks are about a 3 dB noise enhancement [83] and an inability to use efficient multiamplitude constellations. However, differential schemes can benefit from assistance by a channel estimator [46]. An interesting alternative to coherent modulation is *differential amplitude and phase shift keying* (DAPSK) [42, 43, 85, 88], where a spectral efficiency greater than that of DPSK is achieved by using a differential coding of amplitude as well. This requires a nonuniform amplitude distribution. Coherent modulation, however, allows arbitrary signal constellations and is an obvious choice in wired systems where the channel hardly changes with time. In wireless systems the efficiency of coherent modulation makes it an interesting choice when the bit rate is high, as in *digital video broadcast* (DVB) [2, 30].

The channel estimation in wired systems is fairly straightforward and is not discussed in detail below. We concentrate on channel estimation in wireless systems, where the complexity of the estimator is an important design criterion.

There are mainly two problems in the design of channel estimators for wireless OFDM systems. The first problem concerns the choice of how pilot information (data/signals known at the receiver) should be transmitted. This pilot information is needed as a reference for channel estimation. The second problem is the design of an estimator with both low complexity and good channel tracking ability. These two problems are interconnected, since the performance of the estimator depends on how pilot information is transmitted.

## 5.1 Pilot information

Channel estimators usually need some kind of pilot information as a point of reference. A fading channel requires constant tracking, so pilot information has to be transmitted more or less continuously. Decision-directed channel estimation can also be used [119], but even in these types of schemes pilot information has to be transmitted regularly to mitigate error propagation.

To the authors' knowledge, there is very little published on how to transmit pilot informa-

tion in wireless OFDM. However, an efficient way of allowing a continuously updated channel estimate is to transmit pilot symbols instead of data at certain locations of the OFDM time-frequency lattice. This can be viewed as a generalization of *pilot-symbol assisted modulation* (PSAM) in the single carrier case. PSAM in the single carrier case was introduced in [73], and thoroughly analyzed in [17]. An example of this is shown in Figure 5.1, where both scattered and continual pilot symbols are shown. In a preliminary draft of the European DVB standard [1], pilot information is specified to be transmitted on boosted subcarriers, both scattered and as continual pilot carriers. Boosted subcarriers means that pilot information is transmitted at higher power than the data.
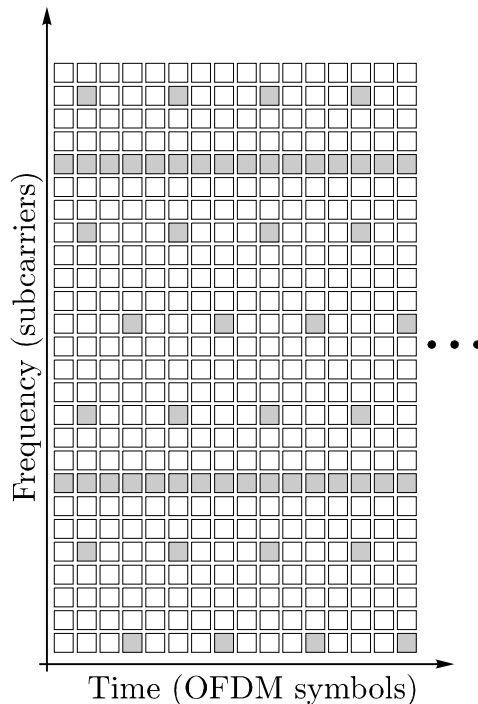


Figure 5.1: An example of pilot information transmitted both scattered and continual on certain subcarriers.

In general, the fading channel can be viewed as a 2-D signal (time and frequency), which is sampled at pilot positions and the channel attenuations between pilots are estimated by interpolation. This enables us to use the 2-D sampling theorem to put limits the density of the pilot pattern [56]. However, as in the single carrier case [17], the pilot pattern should be designed so that the channel is oversampled at the receiver.

## 5.2 Estimator design

Assuming that the pilot pattern is chosen, the optimal linear channel estimator in terms of *mean-squared error* (MSE) is a 2-D Wiener filter. Knowing the statistical properties of the channel, such an estimator can be designed using standard techniques [97]. The combination of high data rates and low bit-error rates necessitates the use of estimators that have both low

complexity and high accuracy. These two constraints on the estimators work against each other. Most estimators with high accuracy, such as the 2-D Wiener filter, have a large computational complexity, while estimators of lower complexity usually produce a less accurate estimate. The art in designing channel estimators is finding a good trade off between complexity and performance.

The issue of reducing the computational complexity, while maintaining most of the performance, has been addressed in several publications. In [56], separable filters are applied instead of a 2-D *finite impulse response* (FIR) filter. The use of separable filters instead of full 2-D filters is a standard technique used to reduce computational complexity in multidimensional signal processing [38]. Using this technique the estimation is first performed in the frequency direction using a 1-D FIR filter, and then in the time direction using a second 1-D FIR filter. This restricts the obtainable 2-D impulse responses to those that are the outer product of two 1-D filters. This results in a small performance loss, but the greatly reduced complexity usually motivates the use of separable filters [56, 92].

A second approach in the reduction of computational complexity is based on using transforms that concentrate the channel power to a few transform coefficients, thus allowing efficient channel estimation to be performed with little effort in the transform domain. Low-complexity estimators of this type, based on both the DFT [9, 19, 39] and on optimal rank reduction [40, 41], have been proposed. This technique usually yield estimators of high performance and low complexity, but may result in an irreducible error floor, unless special care is taken. These effects are analyzed in detail in [39, 41].

A comparative analysis of pilot-based estimators presented in [92] shows that the combination of separable filters and low-rank approximations can give high performance estimators of low complexity, where the greatest portion of the reduced complexity stems from the use of separable filters.

## 5.3   Performance example

Figure 5.2 shows an example on the difference in coded bit-error rate between coherent and differential modulation. The simulations are performed for a wireless 1024 subcarrier OFDM system with a 50-sample cyclic prefix. The channel is Rayleigh-fading with 5% relative Doppler frequency and the system uses trellis-coded modulation with 8 *phase-shift keying* (8-PSK) according to [60]. The differential modulation is performed in the frequency direction, since the frequency correlation is greater than the time correlation [92]. The performance of coherent modulation is presented for both known channel and with a low-complexity estimator [92]. The low-complexity channel estimator uses a 1/16 pilot-symbol density, and requires only 3 multiplications per estimated channel attenuation.

This figure illustrates that coherent modulation with low-complexity channel estimation can outperform differential modulation. Even though the channel correlation in the frequency direction is large in this case, the beginning of an error-floor for the differential modulation is clearly visible for $E_b/N_0$ greater than about 15 dB. This error-floor is of the same type as the one experienced in the single-carrier case when the channel is fading [6].
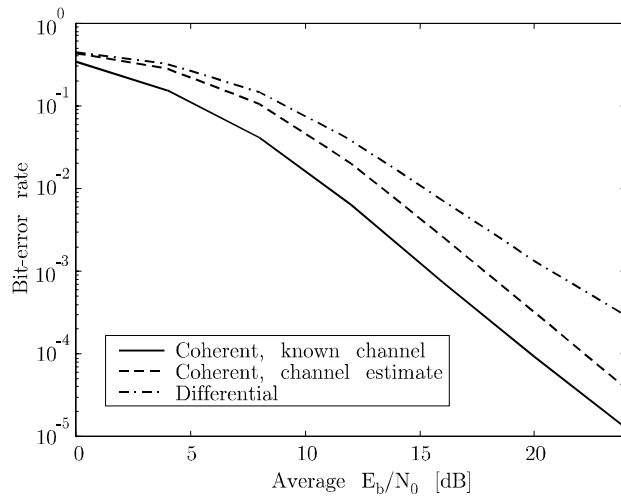
Figure 5.2: An example on the difference between coherent and differential 8-PSK in a Rayleigh-fading environment.

# Chapter 6

# Channel coding

This chapter describes coding in OFDM systems. The coding problem is quite different for the wireless and the wired case. In the latter case the channel is static and techniques like bit loading and multidimensional coding are appropriate. On a fading channel, the main difference between an OFDM system and a single-carrier system is the interleaving. We will give a short overview of coding on both wireless and the wired channels.

## 6.1  Wireless systems

Using a time-domain equalizer it is possible to obtain an $M$-branch diversity if the channel consists of $M$ resolvable paths [118]. In OFDM the equalizer does not give you any diversity, since all subchannels are narrowband and experience flat fading [96]. However, the structure of OFDM offers the opportunity to code across the subcarriers. In [118] it is shown that with an $M$-path channel it is possible to obtain an $M$-branch diversity through coding. Hence, in this diversity context, a multi-carrier system is comparable to a single-carrier system. Besides combating fading, coding has also been proposed to deal with long echoes that causes ISI between subsequent OFDM symbols [110].

The design of codes for OFDM systems on fading channels follows many of the standard techniques. What is special about OFDM is the time-frequency lattice and the possibility to use two dimensions for interleaving and coding. To illustrate how to use this structure we give an overview of two systems: the European DAB standard and a trellis-coded system by Höher. The DAB system uses differential modulation, which avoids channel estimation, while the other system uses a multiamplitude signal constellation, which requires channel estimation.

### 6.1.1  Digital Audio Broadcasting

Digital broadcasting to mobile receivers was under considerable investigation in the late Eighties [5, 69]. The standard for DAB was set in Europe to use OFDM [1], while it is still under investigation in the USA [66]. The European DAB system uses *differential quadrature phase-shift keying* (DQPSK) to avoid channel estimation. An argument for this is based on simple and inexpensive receivers for consumers. The channel encoding process is based on punctured convolutional coding, which allows both equal and unequal error protection [58]. As a mother code, a rate 1/4 convolutional code with constraint length 7 and octal polynomials

(133,171,145,133) is used. The puncturing procedure allows the effective code rate to vary between 8/9 and 1/4.

Interleaving is performed in both time and frequency. The former is a kind of block interleaving after which the bits are mapped to QPSK symbols. The frequency interleaver, working with the QPSK symbols, follows a permutation rule of the 2048 subcarriers. In one of the three transmissions modes, this permutation rule is

$$
\begin{aligned}
\Pi\left(0\right) &= 0 \\
\Pi\left(n\right) &= 13\Pi\left(n-1\right) + 511 \left(\mathrm{mod}\,2048\right), \qquad n = 1,\ldots,2047.
\end{aligned}
$$

This permutation defines the set

$$
\{\Pi\left(0\right), \Pi\left(1\right), \Pi\left(2\right), \ldots, \Pi\left(2047\right)\} = \{0, 511, 1010, \ldots, 1221\}
$$

according to which the interleaving pattern is chosen. After the frequency interleaving, the QPSK symbols are differentially modulated on each subcarrier.

### 6.1.2 Trellis-coded OFDM

As an example of a multiamplitude, coherent, and coded OFDM system, we give a short overview of a system investigated by Höher. The original investigation [56] addresses a digital audio broadcasting scenario, but the concept is more general. Höher's investigation is therefore one of the most referenced papers on OFDM. His system is a power and bandwidth-efficient concatenated coding system for data transmission on time- and frequency-selective mobile fading channels. A concatenated coding is used in conjunction with double interleaving and slow frequency hopping to provide diversity. An overview of the system is depicted in Figure 6.1. The outer codes are *rate-compatible punctured codes* (RCPC) derived from the rate 1/2
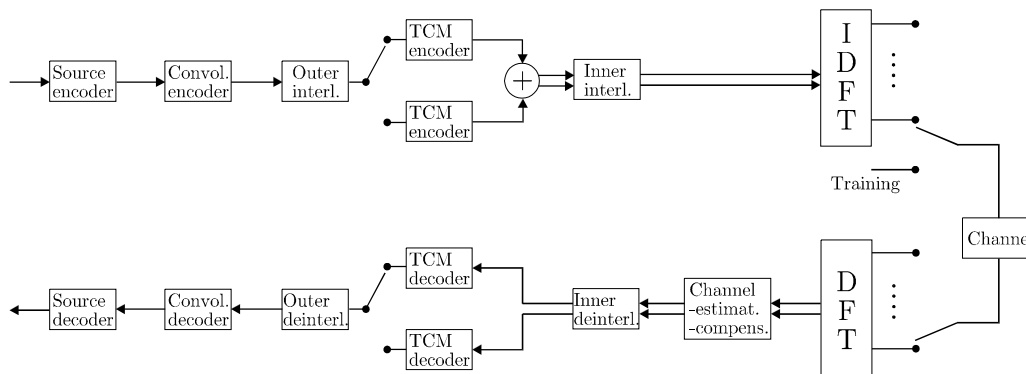


Figure 6.1: Overview of the system investigated by Höher [56].

code $(171, 133)$ with constraint length 7. The outer interleaving scheme is applied to break up error bursts from the inner coding system. Since these bursts are typically much shorter than the fading bursts, the outer interleaving can be much simpler than the inner interleaving.

The inner code is binary *trellis-coded modulation* (TCM) with one-dimensional signal constellation. The reason for this choice is that they were found to provide a good diversity factor

at a very low decoder complexity [73]. The code used is a one-dimensional 8-state code with 4-level (uniform) *pulse-amplitude modulation* (4-PAM). The 4-PAM output symbols are then combined to a 16 symbol *quadrature-amplitude modulation* (16-QAM) constellation and interleaved to break up channel memory. In the receiver the *Viterbi algorithm* (VA) is used for decoding. This algorithm is capable of using the channel state information obtained from a pilot sequence, see Section 5. The decoding is performed by minimizing the metric

$$ J = \sum_n \left| \widehat{h}_n \right|^2 |y_n - x_n|^2 , $$

where $\widehat{h}_n$ is the channel estimate, $y_n$ is the deinterleaved observation after equalization (the real or imaginary part) and $x_n$ is a potential codeword. Because of the outer code, the VA should be modified to provide reliability estimates together with the decoded sequence. This enables soft decoding of the outer code as well. By applying a *soft-output Viterbi algorithm* (SOVA), an improvement of about 2 dB is obtained [56]. Together with inner coding, multicarrier signalling and slow frequency hopping, the interleaver provides dual time/frequency diversity. An example of slow frequency hopping is depicted in Figure 6.2. Each program consists of a
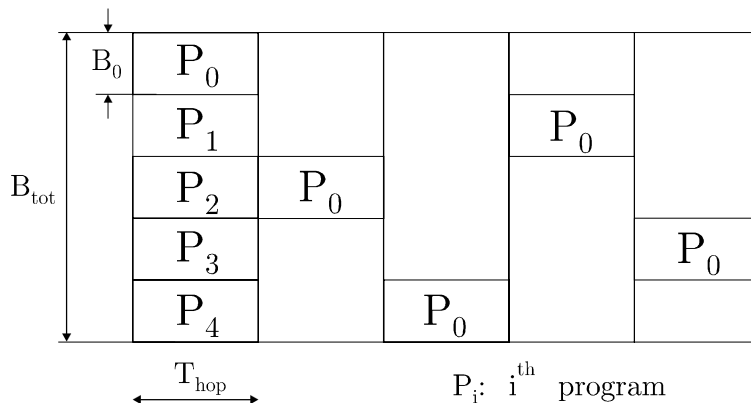


Figure 6.2: Slow frequency hopping. Each program $P_i$ uses a bandwidth $B_0$ and changes frequency band after $T_{hop}$.

number of subcarriers and OFDM symbols; the parameters $B_0$ and $T_{hop}$ are chosen to maximize the diversity of the system. A similar but somewhat more generalized hopping scheme is presented in [7].


### 6.1.3   Other systems

There have been other coded OFDM systems proposed and analyzed in the literature. In [14, 15] an OFDM/FM system is investigated and simulated. OFDM is proposed in Europe as the transmission technique for the new DVB system [2], where a multiresolution scheme is used together with joint source/channel coding [84, 100]. This allows several bit-rates and thereby a graceful degradation of image quality in the fringes of the broadcast area.

### 6.1.4 Coding on fading channels

Codes for fading channels have been investigated for a long time and the search for good codes is still going on. An overview of this subject is found in [103]. Design of codes has been analyzed in [37, 60, 98, 99] and for trellis coded multiple PSK in [33, 34]. Asymmetric PSK constellations are considered in [32] and code design for Rician-fading channels is investigated in [55]. Performance bounds have been derived for Rayleigh-fading channels in [35, 36, 71, 101, 102, 111, 122] and for Rician-fading channels in [47, 104, 105].

Usually performance analysis of codes assumes perfect knowledge of the channel. However, in [16, 53] an analytical method was introduced that allows non-ideal channel information. This was later generalized to include non-ideal interleaving [54, 77]. This method has been used to analyze a coded OFDM system with pilot-based channel estimation on Rayleigh-fading channels [94]. A major benefit of using analytical methods for evaluation of coded systems is that a coded bit-error rate can be obtained quickly after system modifications, without time-consuming simulations.

## 6.2 Wired systems

An important difference between a wired and a wireless system is the characteristics of the channel. In the wired case the channel is often considered stationary, which facilitates a number of techniques to improve the communication system. Channel coding in combination with a technique called bit loading is often employed for this purpose. Multidimensional trellis codes are well suited for the channel coding. When using bit loading the subchannels are assigned individual numbers of bits according to their respective SNRs. An OFDM-based communication system using bit loading is often referred to as a DMT system.

### 6.2.1 Bit loading

Bit loading is a technique that is used for multicarrier systems operating on stationary channels [13]. A stationary channel makes it possible to measure the SNR on each subchannel and assign individual numbers of transmitted bits. A subchannel with high SNR thus transmits more bits than a subchannel with low SNR. Figure 6.3 shows a schematic picture of SNR and how the number of bits on each subchannel vary accordingly.
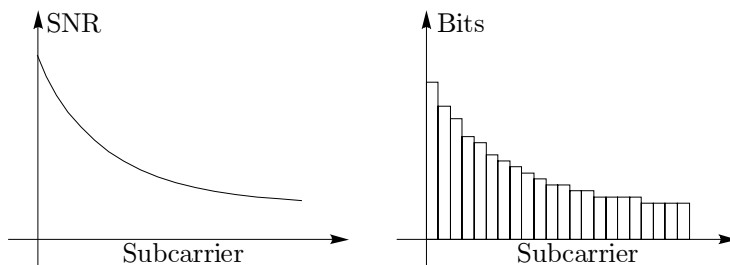


Figure 6.3: Channel SNR (left) and corresponding number of bits on each subcarrier (right).

When performing bit loading one usually optimizes for either high data rate, low average transmitting energy, or low error probability. Typically two of these are kept constant and the

third is the goal for the optimization. Which parameter should be optimized depends on the system, its environment, and its application.

When there is only one system operating on a cable, this system neither interferes with nor is interfered by other systems. This means that controlling the transmitting power to reduce crosstalk is not necessary. Given a data rate and a bit-error probability, whatever transmission energy needed to achieve these goals can be used (within reasonable limits). In a multi-system environment, where there are several systems transmitting in the same cable, the problem is more complicated, since the systems experience crosstalk. The level of crosstalk is proportional to the transmitting power in the systems, see (3.1) and (3.2). It is therefore desirable to have an equal transmission power in all systems, to obtain equal disturbance situations. In a multi-system environment the average transmitting power is usually fixed, and the optimization is for either high data rate or low bit-error rate.

## 6.2.2  Bit-loading algorithms

There are several techniques for bit loading in DMT systems and some of these are described in [13, 21, 45, 107]. As mentioned earlier, there are several parameters that one can optimize for. Most algorithms optimize for high data rate or low bit-error rate.

Given a certain data rate and an energy constraint, the Hughes-Hartogs algorithm provides the bit-loading factors that yield minimal bit-error rate, see *e.g.* [13]. The idea behind the Hughes-Hartogs algorithm is to assign one bit at a time to the subchannels. The algorithm calculates the energy cost to send one bit more on each subchannel. The subchannel with the smallest energy cost is then assigned the bit. This procedure is repeated until a desired bit rate is obtained. Chow has showed that complexity of the Hughes-Hartogs algorithm is proportional to the number of subchannels and the number of bits transmitted in a DMT frame [21]. He also suggests a suboptimal algorithm of lower complexity in [21].

An algorithm that maintains an equal bit-error probability over all subchannels, given a data rate and an energy constraint, is presented by Fischer in [45].

A suboptimal way of performing bit loading to achieve a high data rate, while maintaining a constant symbol-error probability across all subchannels, is presented by Tu [107]. In his algorithm the bit-loading factors are calculated according to

$$b_k = \log_2 \left( \frac{3E_k g_k \gamma_d}{2K\sigma_k^2} + 1 \right) - \log_2 C, \tag{6.1}$$

where $b_k$ is the number of bits carried (bit-loading factor) on subcarrier $k$, $E_k$ the average symbol transmission energy, $g_k$ the channel attenuation, and $\sigma_k^2$ the noise variance. The coding gain is denoted $\gamma_d$ and the constellation expansion factor, due to coding, is denoted $C$. Further, to obtain a desired symbol-error rate of $P_e$, the design constant $K$ is chosen to

$$K = \left[ Q^{-1} \left( \frac{P_e}{N_e} \right) \right]^2, \tag{6.2}$$

where $N_e$ is the number of nearest neighbors.

Expression (6.1) can be viewed as the union bound for a QAM-constellation, with some modifications for coding, where $K$ is the SNR required to obtain an error probability $P_e$. The channel SNR (including coding), $3E_k g_k \gamma_d / 2\sigma_k^2$, is divided by the SNR required to transmit one

bit. Finally, the number of bits needed in the coding, $\log_2 C$, is subtracted to get the number of bits carried by subchannel $k$.

If the number of systems transmitting in a cable vary, the amount of crosstalk will vary accordingly. To handle the situation where the number of transmitting systems vary one can either do the bit loading for a worst case or employ adaptive bit loading. Chow [21] presents such an adaptive algorithm, called the bit-swap algorithm, which is designed for the case when a fixed data rate is specified.

When trying to maximize the data rate with a constant transmitting power, it is optimal to allow bit-loading factors to span a continuous range of values. Tu presents some results in [107] on how the granularity of bit-loading factors affects the obtained data-rate in such a system. One way to get non-integer bit-loading factors is to use multidimensional codes. Multidimensional codes allow a fractional number of bits per 2-D symbol to be transmitted on each subchannel. For 2-D, 4-D, and 8-D codes the granularities become 1 bit, 0.5 bits, and 0.25 bits per 2-D symbol, respectively. Another technique, referred to as energy loading, is to allow some sort of fine tuning of the transmitted energy on the subchannels, *i.e.*, adjusting the energy $E_k$ in (6.1) so that it corresponds to one of the supported bit-loading factors. However, energy loading only works if the tuning is small, which requires many bit-loading factors, and a side effect is that a more complex signal constellation mapper/demapper is required.

### 6.2.3   Channel coding

Coding in DMT has been analyzed in *e.g.*, [12, 123]. A typical coding scheme for DMT consists of an outer code, an interleaver, and an inner code. Due to the type of applications that DMT is designed to carry, see Section 3.2, it is appealing to keep a low delay between transmitter and receiver. This limits the interleaving depth and affects the choice of error-correcting codes.

The coding scheme analyzed in [12] uses an outer Reed-Solomon code and an inner trellis code. The Reed-Solomon code and interleaving are designed to reduce errors due to impulse noise. By using only one coder that codes across subcarriers, the delay is small compared to the case where one trellis code is used for each subcarrier. This is due to the Viterbi decoder's need for a certain decision depth to make a good decision. In the investigated system the, amount of data sent in one DMT frame is enough for the Viterbi algorithm to make a decision.

Multidimensional codes are well suited for DMT systems. By using several 2-D constellations on different subchannels it is easy to create multidimensional constellations. As described earlier, the multidimensional codes allow fractional bits to be transmitted, which reduces the granularity of the bit-loading factors.

# Chapter 7

# Discussion

This section is both a discussion and a summary of the material presented earlier in this report.

One of the major advantages of OFDM is its robustness against multipath propagation. Hence, its typical applications are in tough radio environments. OFDM is also suitable in single frequency networks, since the signals from other transmitters can be viewed as echoes, *i.e.*, multipath propagation. This means that it is favorable to use OFDM in broadcasting applications, such as DAB and DVB. The use of OFDM in multiuser systems has gained an increasing interest the last few years. The downlink in those systems is similar to broadcasting, while the uplink puts high demands on *e.g.*, synchronization. The future of OFDM as a transmission technique for multiuser systems depends on how well these problems can be solved.

In wired systems the structure of OFDM offers the possibility of efficient bit loading. By allocating a different number of bits to different subchannels, depending on their individual SNRs, efficient transmission can be achieved. Although other systems have been proposed, OFDM is the dominating technique on *e.g.*, digital subscriber lines. Note that OFDM often goes under the name DMT when used in wired systems with bitloading.

There are also problems associated with OFDM system design. The two main obstacles when using OFDM are the high peak-to-average-power ratio and synchronization. The former puts high demands on linearity in amplifiers. Synchronization errors, in both time and frequency, destroy the orthogonality and cause interference. By using a cyclic prefix, the timing requirements are somewhat relaxed, so the biggest problems are due to high frequency synchronization demands. Degradation due to frequency errors can be caused both by differences in local oscillators and by Doppler shifts. A great deal of effort is therefore spent on designing accurate frequency synchronizers for OFDM.

As in any digital communication system, there are two alternatives for modulation: coherent or differential. The European DAB system uses differential QPSK, while the proposed scheme for DVB is coherent 64-QAM. Differential PSK is suitable for low data rates and gives simple and inexpensive receivers, which is important for portable consumer products like DAB receivers. However, in DVB the data rate is much higher and low bit-error rates are difficult to obtain with differential PSK. A natural choice for DVB is therefore multiamplitude schemes. Due to the structure in OFDM, it is easy to design efficient channel estimators and equalizers. This is one of the appealing properties of OFDM which should be exploited to achieve high spectral efficiency.

Coding in wireless OFDM systems does not differ much from coding in wireless single-carrier

systems. The main difference is that interleaving in OFDM allows symbols to be spread in both time and frequency. The possibility to interleave in frequency overcomes the drawback of not obtaining diversity from the equalizer. Since each subchannel experiences flat fading, code design and performance analysis developed for flat fading channels can be used. Decoding can be performed with a Viterbi decoder, where the metric depends on the (estimated) channel attenuations. This means that symbols are weighed with their respective channel strength. This reduces the effect of errors caused by symbols transmitted during a fade.

## Acknowledgements

# Appendix A

# Time-frequency lattice

In this appendix we give a brief overview of the effects of pulse shaping. We only consider time and frequency dispersion and exclude channel noise in this analysis. We describe the OFDM signal as

$$s(t) = \sum_{k,l} x_{k,l} \phi_{k,l}(t), \qquad \text{(A.1)}$$

where the functions $\phi_{k,l}(t)$ are translations of a prototype function $p_t(t)$:

$$\phi_{k,l}(t) = p_t\left(t - l\tau_0\right) e^{j2\pi k\nu_0 t}. \qquad \text{(A.2)}$$

This allows us to interpret the pulse shaping problem. The receiver uses the functions $\psi_{k,l}(t)$ that are translations of a (possibly different) prototype function $p_r(t)$:

$$\psi_{k,l}(t) = p_r\left(t - l\tau_0\right) e^{j2\pi k\nu_0 t}.$$

In OFDM these functions fulfil

$$\langle \phi_{k,l}(t), \psi_{k',l'}(t) \rangle = \delta\left[k - k', l - l'\right],$$

where $\langle \cdot, \cdot \rangle$ denotes the Euclidean inner product [109]. Hence, the transmitter and receiver functions are bi-orthogonal [109]. This simplifies the receiver since

$$\langle s(t), \psi_{k,l}(t) \rangle = \int_{-\infty}^{\infty} s(t)\psi_{k,l}^*(t)dt = x_{k,l}.$$

However, a time or frequency dispersive channel destroys this orthogonality. By carefully choosing $p_t(t)$ and $p_r(t)$, the effects of the loss of orthogonality can be kept low. An OFDM system must be sufficiently resistant to both time and frequency dispersion. The former can dealt with by introducing a guard space (usually in the form of a cyclic prefix), while the latter is often approached by pulse shaping. In systems with a cyclic prefix and no pulse shaping, the functions $p_t(t)$ and $p_r(t)$ are chosen as the rectangular pulse, although of different lengths. The receiver prototype function $p_r(t)$ in this case is shorter than the transmitter prototype function $p_t(t)$, which corresponds to the removal of the cyclic prefix.

A common propagation model is obtained by assuming that the channel consists of a number of elementary paths [83], where each path is described by a delay, a frequency offset, and a

complex attenuation. Thus by investigating the effects of a static delay and frequency offset, the sensitivity to a fading multipath channel can be evaluated [68]. This analysis can be made with the cross-ambiguity function [51] of the prototype functions $p_t(t)$ and $p_r(t)$

$$A(\tau, f) \triangleq \int_{-\infty}^{\infty} p_t(t) p_r^*(t - \tau) e^{-j2\pi ft} dt,$$

which can be viewed as a crosscorrelation function in the time-frequency plane. The bi-orthogonality of $\phi_{k,l}$ and $\psi_{k,l}(t)$ requires that

$$
\begin{aligned}
\langle \phi_{k,l}(t), \psi_{k+m,l+n}(t) \rangle &= e^{-j2\pi ml\tau_0} \int_{-\infty}^{\infty} p_t(t) p_r^*(t - n\tau_0) e^{-j2\pi m\nu_0 t} dt \qquad \text{(A.3)} \\
&= e^{-j2\pi ml\tau_0} A(n\tau_0, m\nu_0) = \delta[n, m].
\end{aligned}
$$

This is a condition on the samples of the cross-ambiguity function at positions $(n\tau_0, m\nu_0)$. The cross-ambiguity function should be zero for all $(n, m) \neq (0, 0)$, but a delay or frequency offset will destroy the ortogonality since $A(\tau, f)$ is not sampled at its zeros. With a delay $\Delta\tau$ and a frequency offset $\Delta\nu$, the signal power is $|A(\Delta\tau, \Delta\nu)|^2$ and the interference power can be upper bounded by $1 - |A(\Delta\tau, \Delta\nu)|^2$ [75]. This bounds the *signal-to-interference ratio* (SIR) from below as

$$\text{SIR} \geq \frac{|A(\Delta\tau, \Delta\nu)|^2}{1 - |A(\Delta\tau, \Delta\nu)|^2}.$$

Thus, the cross-ambiguity function is a measure of the interference in the system caused by a delay or a frequency offset. In [68] a prototype function is created, which is claimed to have a near-optimum cross-ambiguity function. The cross-ambiguity function for a rectangular pulse in a system with cyclic prefix is shown in Figure A.1. Note that the system is insensitive to a
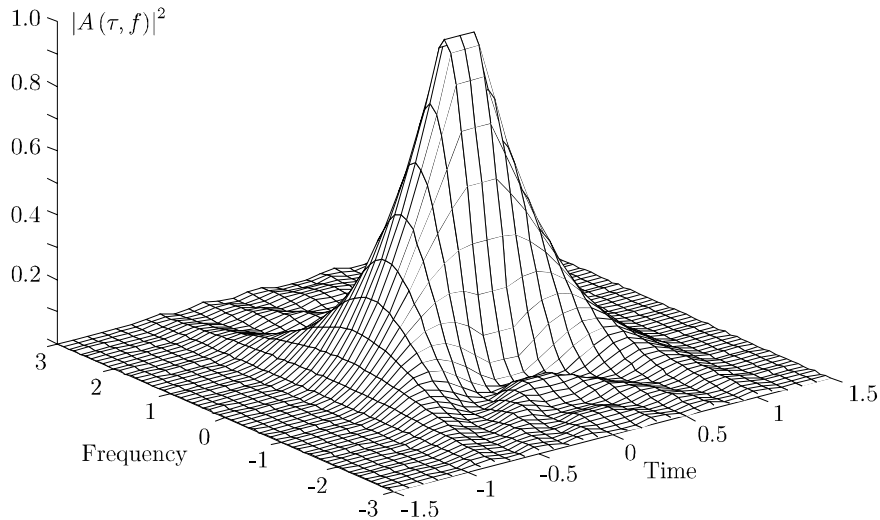


Figure A.1: Ambiguity function for a rectangular pulse and cyclic prefix with lengths $\tau_0 = 1.2$ and $T_{cp} = 0.2$, respectively.

time delay less than $T_{cp} = 0.2$, since the cross-ambiguity function is flat at the top.

The main problem with choosing $p(t)$ as a rectangular pulse is that it is not well localized in frequency. Denote the time and frequency widths, respectively, of the unit energy signal $p(t)$ by

$$(\Delta t)^2 = \int_{-\infty}^{\infty} t^2 \, |p(t)|^2 \, dt$$

$$(\Delta f)^2 = \int_{-\infty}^{\infty} f^2 \, |P(f)|^2 \, df,$$

where $P(f)$ is the Fourier transform of $p(t)$. Then $\Delta t = \tau_0/\sqrt{12}$ and $\Delta f = \infty$ for the rectangular pulse. This frequency spread of energy is the reason for ICI in the case of transmission over frequency dispersive channels [51]. Thus, other pulses have been sought to overcome this problem. Since the Gaussian pulse $p(t) = e^{-\pi t^2}$ has a minimal time-bandwidth product [26], it has been used to form suitable functions [51, 68]. Prolate spheroidal wave functions [67] have also been used to minimize out-of-band energy in pulses under certain conditions [52, 108].

# Bibliography

[1] Radio broadcasting systems; Digital Audio Broadcasting (DAB) to mobile, portable and fixed receivers. ETS 300 401, ETSI – European Telecommunications Standards Institute, Valbonne, France, Feb. 1995.

[2] Digital broadcasting systems for television, sound and data services. European Telecommunications Standard, prETS 300 744 (Draft, version 0.0.3), Apr. 1996.

[3] Transmission and reception. Technical Report GSM Recommendation 05.05, version 3.11.0, ETSI, Valbonne, France, Mar. 1996.

[4] Working document towards ETR/SMG-50402 selection procedures for the choice of radio transmission technologies of the universal mobile telecommunications system (UMTS). Technical Report DTR/SMG-50402, ETSI, Valbonne, France, 1996.

[5] M. Alard and R. Lassalle. Principles of modulation and channel coding for digital broadcasting for mobile receivers. *EBU Review – Technical*, (224):168–190, Aug. 1987.

[6] J. B. Andersen and B. L. Andersen. First-order frequency selective effects on phase modulations in a fading channel. Technical Report COST 231 TD(91), EURO–COST, Firenze, Jan. 1991.

[7] J.-J. van de Beek, O. Edfors, P. O. Börjesson, M. Wahlqvist, and C. Östberg. A conceptual study of OFDM-based multiple access schemes: Part 2 – Channel estimation in the uplink. Technical Report Tdoc 116/96, ETSI STC SMG2 meeting no 18, Helsinki, Finland, May 1996.

[8] J.-J. van de Beek, O. Edfors, P. O. Börjesson, M. Wahlqvist, and C. Östberg. A conceptual study of OFDM-based multiple access schemes: Part 3 – Performance evaluation of a coded system. Technical Report Tdoc 166/96, ETSI STC SMG2 meeting no 19, Düsseldorf, Germany, Sept. 1996.

[9] J.-J. van de Beek, O. Edfors, M. Sandell, S. K. Wilson, and P. O. Börjesson. On channel estimation in OFDM systems. In *Proc. IEEE Vehic. Technol. Conf.*, volume 2, pages 815–819, Chicago, IL, July 1995.

[10] J.-J. van de Beek, M. Sandell, and P. O. Börjesson. ML estimation of timing and frequency offset in multicarrier systems. Research Report TULEA 1996:09, Division of Signal Processing, Luleå University of Technology, 1996.

[11] J.-J. van de Beek, M. Sandell, M. Isaksson, and P. O. Börjesson. Low-complex frame synchronization in OFDM systems. In *Proc. Int. Conf. Universal Personal Commun.*, pages 982–986, Tokyo, Japan, Nov. 1995.

[12] D. Bengtsson and D. Landström. Coding in a discrete multitone modulation system. Master's thesis, Luleå University of Technology, Apr. 1996.

[13] J. A. C. Bingham. Multicarrier modulation for data transmission: An idea whose time has come. *IEEE Commun. Mag.*, 28(5):5–14, May 1990.

[14] E. F. Casas and C. Leung. OFDM for data communication over mobile radio FM channels – Part I: Analysis and experimantal results. *IEEE Trans. Commun.*, 39(5):783–793, May 1991.

[15] E. F. Casas and C. Leung. OFDM for data communication over mobile radio FM channels – Part II: Performance improvement. *IEEE Trans. Commun.*, 40(4):680–683, Apr. 1992.

[16] J. Cavers and P. Ho. Analysis of the error performance of trellis-coded modulation in Rayleigh-fading channels. *IEEE Trans. Commun.*, 40(1):74–83, Jan. 1992.

[17] J. K. Cavers. An analysis of pilot-symbol assisted modulation for Rayleigh-fading channels. *IEEE Trans. Vehic. Technol.*, 40(4):686–693, Nov. 1991.

[18] R. W. Chang. Synthesis of band-limited orthogonal signals for multichannel data transmission. *Bell System Tech. J.*, 45:1775–1796, Dec. 1966.

[19] A. Chini. *Multicarrier modulation in frequency selective fading channels*. PhD thesis, Carleton University, Ottawa, Canada, 1994.

[20] A. Chini, M. S. El-Tanany, and S. A. Mahmoud. Transmission of high rate ATM packets over indoor radio channels. *IEEE J. Select. Areas Commun.*, 14(3):469–476, Apr. 1996.

[21] P. S. Chow. *Bandwidth optimized digital transmission techniques for spectrally shaped channels with impulse noise*. PhD thesis, Stanford University, CA, May 1993.

[22] P. S. Chow, N. Al-Dhahir, and J. M. Cioffi. A multicarrier E1-HDSL transceiver system with coded modulation. *Eur. Trans. Telecommun. Rel. Technol.*, 4(3):257–266, May 1993.

[23] P. S. Chow, J. M. Cioffi, and J. A. C. Bingham. A practical discrete multitone transceiver loading algorithm for data transmission over spectrally shaped channels. *IEEE Trans. Commun.*, 43(2/3/4):773–775, Feb. 1995.

[24] L. J. Cimini. Analysis and simulation of a digital mobile channel using orthogonal frequency-division multiplexing. *IEEE Trans. Commun.*, COM-33(7):665–675, July 1985.

[25] F. Classen and H. Meyr. Frequency synchronization algorithms for OFDM systems suitable for communication over frequency-selective fading channels. In *Proc. IEEE Vehic. Technol. Conf.*, volume 3, pages 1655–1659, Stockholm, Sweden, June 1994.

[26] L. Cohen. *Time-frequency analysis*. Prentice-Hall, New Jersey, 1995.

[27] J. W. Cook. Wideband impulsive noise survey of the access network. *BT Technol. Journ.*, 11(3):155–162, July 1993.

[28] F. Daffara and O. Adami. A new frequency detector for orthogonal multicarrier transmission techniques. In *Proc. IEEE Vehic. Technol. Conf.*, volume 2, pages 804–809, Chicago, IL, July 1995.

[29] F. Daffara and A. Chouly. Maximum-likelihood frequency detectors for orthogonal multicarrier systems. In *Proc. Intern. Conf. Commun.*, pages 766–771, Geneva, Switzerland, May 1993.

[30] T. de Couasnon, R. Monnier, and J. B. Rault. OFDM for digital TV broadcasting. *Signal Proc.*, 39(1–2):1–32, Sept. 1994.

[31] R. Dinis, P. Montezuma, and A. Gusmão. Performance trade-offs with quasi-linearly amplified OFDM through a two-branch combining technique. In *Proc. IEEE Vehic. Technol. Conf.*, volume 2, pages 899–903, Atlanta, GA, Apr. 1996.

[32] D. Divsalar and M. K. Simon. Trellis-coded modulation for 4800-9600 bits/s transmission over a fading mobile satellite channel. *IEEE J. Select. Areas Commun.*, SAC-5(2):162–175, Feb. 1987.

[33] D. Divsalar and M. K. Simon. The design of trellis-coded MPSK for fading channels: Performance criteria. *IEEE Trans. Commun.*, 36(9):1004–1012, Sept. 1988.

[34] D. Divsalar and M. K. Simon. The design of trellis-coded MPSK for fading channels: Set partitioning for optimum code design. *IEEE Trans. Commun.*, 36(9):1013–1021, Sept. 1988.

[35] D. Divsalar and M. K. Simon. Multiple-symbol differential detection of MPSK. *IEEE Trans. Commun.*, 38(3):300–308, Mar. 1990.

[36] D. Divsalar and M. K. Simon. Maximum-likelihood differential detection of uncoded and trellis-coded amplitude phase modulation over AWGN and fading channels – Metrics and performance. *IEEE Trans. Commun.*, 42(1):76–89, Jan. 1994.

[37] J. Du and B. Vucetic. Trellis-coded 16-QAM for fading channels. *Eur. Trans. Telecommun. Rel. Technol.*, 4(3):101–107, May 1993.

[38] D. E. Dudgeon and R. M. Mersereau. *Multidimensional digital signal processing.* Prentice–Hall, Englewood Cliffs, NJ, 1984.

[39] O. Edfors, M. Sandell, J.-J. van de Beek, S. K. Wilson, and P. O. Börjesson. Analysis of DFT-based channel estimators for OFDM. Research Report TULEA 1996:17, Div. of Signal Processing, Luleå University of Technology, Sept. 1996.

[40] O. Edfors, M. Sandell, J.-J. van de Beek, S. K. Wilson, and P. O. Börjesson. OFDM channel estimation by singular value decomposition. In *Proc. IEEE Vehic. Technol. Conf.*, pages 923–927, Atlanta, GA, Apr. 1996.

[41] O. Edfors, M. Sandell, J.-J. van de Beek, S. K. Wilson, and P. O. Börjesson. OFDM channel estimation by singular value decomposition. Research Report TULEA 1996:18, Div. of Signal Processing, Luleå University of Technology, Sept. 1996.

[42] V. Engels and H. Rohling. Differential modulation techniques for a 34 MBit/s radio channel using orthogonal frequency-division multiplexing. *Wireless Pers. Commun.*, 2(1–2):29–44, 1995.

[43] V. Engels and H. Rohling. Multilevel differential modulation techniques (64-DAPSK) for multicarrier transmission systems. *Eur. Trans. Telecommun. Rel. Technol.*, 6(6):633–640, Nov. 1995.

[44] K. Fazel. Performance of convolutionally coded CDMA/OFDM in a frequency-time selective fading channel and its near-far resistance. In *Proc. Intern. Conf. Commun.*, volume 3, pages 1438–1442, New Orleans, LA, Nov. 1994.

[45] R. F. Fischer and J. B. Huber. A new loading algorithm for discrete multitone transmission. In *Proc. Globecom*, London, UK, 1996.

[46] P. Frenger and A. Svensson. A decision-directed coherent detector for OFDM. In *Proc. IEEE Vehic. Technol. Conf.*, volume 3, pages 1584–1588, Atlanta, GA, Apr. 1996.

[47] F. Gagnon and D. Haccoun. Bounds on the error performance of coding for nonindependent Rician-fading channels. *IEEE Trans. Commun.*, 40(2):351–360, Feb. 1992.

[48] M. Ghosh. Analysis of the effect of impulse noise on multicarrier and single-carrier QAM systems. *IEEE Trans. Commun.*, 44(2):145–147, Feb. 1996.

[49] R. Gross and D. Veeneman. Clipping distortion in DMT ADSL systems. *Electron. Lett.*, 29(24):2080–2081, Nov. 1993.

[50] M. Gudmundson and P.-O. Andersson. Adjacent channel interference in an OFDM system. In *Proc. IEEE Vehic. Technol. Conf.*, volume 2, pages 918–922, Atlanta, GA, Apr. 1996.

[51] R. Haas. *Application des transmissions à porteuses multiples aux communications radio mobiles*. Phd. thesis, Ecole National Supérieure des Télécommunications, Paris, France, Jan. 1996. In English.

[52] P. H. Halpern. Optimum finite duration Nyquist signals. *IEEE Trans. Commun.*, COM-27(6):884–888, June 1979.

[53] P. Ho, J. Cavers, and J. Varaldi. The effects of constellation density on trellis-coded modulation in fading channels. *IEEE Trans. Vehic. Technol.*, 42(3):318–325, Aug. 1993.

[54] P. Ho and D. Fung. Error performance of multiple-symbol differential detection of PSK signals transmitted over correlated Rayleigh-fading channels. *IEEE Trans. Commun.*, 40(10):1566–1569, Oct. 1992.

[55] J. Huang and L. L. Campbell. Trellis-coded MDPSK in correlated and shadowed Rician-fading channels. *IEEE Trans. Commun.*, 40(4):786–797, Nov. 1991.

[56] P. Höher. TCM on frequency-selective land-mobile fading channels. In *Proc. Tirrenia Int. Workshop Digital Commun.*, Tirrenia, Italy, Sept. 1991.

[57] P. Höher. A statistical discrete-time model for the WSSUS multipath channel. *IEEE Trans. Commun.*, 41(4):461–468, Nov. 1992.

[58] P. Höher, J. Hagenauer, E. Offer, C. Rapp, and H. Schulze. Performance of an RCPC-coded OFDM-based digital audio braodcasting (DAB) system. In *Proc. Globecom*, volume 1, pages 40–46, 1991.

[59] W. C. Jakes. *Microwave mobile communications*. Classic Reissue. IEEE Press, Piscataway, New Jersey, 1974.

[60] S. H. Jamali and T. Le-Ngoc. A new 4-state 8-PSK TCM scheme for fast fading, shadowed mobile radio channels. *IEEE Trans. Vehic. Technol.*, 40(1):216–222, Feb. 1991.

[61] A. Jones and T. Wilkinson. Combined coding for error control and increased robustness to system nonlinearities in OFDM. In *Proc. IEEE Vehic. Technol. Conf.*, volume 2, pages 904–908, Atlanta, GA, Apr. 1996.

[62] A. Jones, T. Wilkinson, and S. Barton. Block coding scheme for reduction of peak to mean envelope power ratio of multicarrier transmission schemes. *Electron. Lett.*, 30(25):2098–2099, Dec. 1994.

[63] I. Kalet. The multitone channel. *IEEE Trans. Commun.*, 37(2):119–124, Feb. 1989.

[64] I. Kalet and S. Shamai. On the capacity of a twisted-wire pair: Gaussian model. *IEEE Trans. Commun.*, 38(3):379–383, Mar. 1990.

[65] K. W. Kang, J. Ann, and H. S. Lee. Decision-directed maximum-likelihood estimation of OFDM frame synchronization offset. *Electron. Lett.*, 30(25):2153–2154, Dec. 1994.

[66] T. Keller *et al.* Report on digital audio radio laboratory tests. Technical report, Electronic Industries Association, May 1995.

[67] H. J. Landau and H. O. Pollak. Prolate spheriodal wave functions, Fourier analysis and uncertainty – III: The dimension of the space of essentially time- and band-limited signals. *Bell System Tech. J.*, 41:1295, 1962.

[68] B. Le Floch, M. Alard, and C. Berrou. Coded orthogonal frequency-division multiplexing. *Proc. IEEE*, 83(6):982–996, June 1995.

[69] B. Le Floch, R. Halbert-Lassalle, and D. Castelain. Digital sound broadcasting to mobile receivers. *IEEE Trans. Consumer Electronics*, 35(3):493–503, Aug. 1989.

[70] B. Marti. European activities on digital television broadcasting – from company to cooperative projects. *EBU Review – Technical*, (256):20–29, 1993.

[71] R. G. McKay, P. J. McLane, and E. Biglieri. Error bounds for trellis-coded MPSK on a fading mobile satellite channel. *IEEE Trans. Commun.*, 39(12):1750–1761, Dec. 1991.

[72] M. Moeneclaey and M. van Bladel. Digital HDTV broadcasting over the CATV distribution system. *Signal Proc.: Image Commun.*, 5(5–6):405–415, Dec. 1993.

[73] M. L. Moher and J. H. Lodge. TCMP – A modulation and coding strategy for Rician-fading channels. *IEEE J. Select. Areas Commun.*, 7(9):1347–1355, Dec. 1989.

[74] P. Moose. A technique for orthogonal frequency-division multiplexing frequency offset correction. *IEEE Trans. Commun.*, 42(10):2908–2914, Oct. 1994.

[75] A. Müller. OFDM transmission over time-variant channels. In *Proc. Int. Broadc. Conv.*, number 397, pages 533–538, Amsterdam, Netherlands, Sept. 1994.

[76] J. Nilsson. Coding to control the signal waveform in M-ary PSK multicarrier communications. In *Proc. Radioveten. Konf.*, pages 658–662, Luleå, Sweden, June 1996.

[77] R. van Nobelen and D. P. Taylor. Analysis of the pairwise error probability of noninterleaved codes on the Rayleigh-fading channel. *IEEE Trans. Commun.*, 44(4):456–463, Apr. 1996.

[78] A. Oppenheim and R. Schafer. *Discrete-time signal processing*. Prentice-Hall, 1989.

[79] A. Peled and A. Ruiz. Frequency domain data transmission using reduced computational complexity algorithms. In *Proc. IEEE Int. Conf. Acoust., Speech, Signal Processing*, pages 964–967, Denver, CO, 1980.

[80] T. Pollet and M. Moeneclaey. Synchronizability of OFDM signals. In *Proc. Globecom*, volume 3, pages 2054–2058, Singapore, Nov. 1995.

[81] T. Pollet, P. Spruyt, and M. Moeneclaey. The BER performance of OFDM systems using non-synchronized sampling. In *Proc. Globecom*, volume 1, pages 253–257, San Francisco, CA, Nov. 1994.

[82] T. Pollet, M. van Bladel, and M. Moeneclaey. BER sensitivity of OFDM systems to carrier frequency offset and Wiener phase noise. *IEEE Trans. Commun.*, 43(2/3/4):191–193, Feb/Mar/Apr 1995.

[83] J. Proakis. *Digital communications*. Prentice-Hall, 3rd edition, 1995.

[84] K. Ramchandran, A. Ortega, K. M. Uz, and M. Vetterli. Multiresolution broadcast for digital HDTV using joint source/channel coding. *IEEE J. Select. Areas Commun.*, 11(1):6–23, Jan. 1993.

[85] C. Reiners and H. Rohling. Multicarrier transmission technique in cellular mobile communication systems. In *Proc. IEEE Vehic. Technol. Conf.*, pages 1645–1649, Stockholm, Sweden, June 1994.

[86] J. Rinne and M. Renfors. The behaviour of orthogonal frequency-division multiplexing in an amplitude limiting channel. In *Proc. IEEE Vehic. Technol. Conf.*, volume 1, pages 381–385, New Orleans, LA, May 1994.

[87] H. Rohling, K. Brüninghaus, and T. Müller. Performance of coherent OFDM-CDMA for broadband mobile communication. In *Proc. RACE Mobile Commun. Summit*, pages 263–269, Cascais, Nov. 1995.

[88] H. Rohling and R. Grünheid. Multicarrier transmission technique in mobile communication systems. In *Proc. RACE Mobile Commun. Summit*, pages 270–276, Cascais, Nov. 1995.

[89] M. Russell and G. Stüber. Interchannel interference analysis of OFDM in a mobile environment. In *Proc. IEEE Vehic. Technol. Conf.*, volume 2, pages 820–824, Chicago, IL, July 1995.

[90] M. Sablatash. Transmission of all-digital advanced television: State of the art and future directions. *IEEE Trans. Broadc.*, 40(2):102–121, June 1994.

[91] B. R. Saltzberg. Performance of an efficient parallel data transmission system. *IEEE Trans. Commun.*, COM-15(6):805–811, Dec. 1967.

[92] M. Sandell and O. Edfors. A comparative study of pilot-based channel estimators for wireless OFDM. Research Report TULEA 1996:19, Div. of Signal Processing, Luleå University of Technology, Sept. 1996.

[93] M. Sandell, J.-J. van de Beek, and P. O. Börjesson. Timing and frequency synchronization in OFDM systems using the cyclic prefix. In *Intern. Symp. Synch.*, pages 16–19, Essen, Germany, Dec. 1995.

[94] M. Sandell, S. K. Wilson, and P. O. Börjesson. Performance analysis of coded OFDM on fading channels with non-ideal interleaving and channel knowledge. Research Report TULEA 1996:20, Div. of Signal Processing, Luleå University of Technology, Sept. 1996.

[95] G. Santella. OFDM with guard interval and subchannel equalization in a 2-resolution transmission scheme for digital television broadcasting. In *Proc. Intern. Conf. Commun.*, volume 1, pages 374–380, New Orleans, LA, May 1994.

[96] H. Sari, G. Karam, and I. Jeanclaude. Transmission techniques for digital terristrial TV broadcasting. *IEEE Commun. Mag.*, 33(2):100–109, Feb. 1995.

[97] L. L. Scharf. *Statistical signal processing: Detection, estimation, and time series analysis.* Addison-Wesley, 1991.

[98] C. Schlegel. Trellis-coded modulation on time-selective fading channels. *IEEE Trans. Commun.*, 42(2/3/4):1617–1627, 1994.

[99] C. Schlegel and D. J. Costello. Bandwidth efficient coding for fading channels: Code construction and performance analysis. *IEEE J. Select. Areas Commun.*, 7(9):1356–1368, Dec. 1989.

[100] W. F. Schreiber. Advanced television systems for terristrial broadcasting: Some problems and some proposed solutions. *Proc. IEEE*, 83(6):958–981, June 1995.

[101] M. K. Simon and D. Divsalar. The performance of trellis-coded multilevel DPSK on a fading mobile satellite channel. *IEEE Trans. Vehic. Technol.*, 37(2):78–91, May 1988.

[102] S. B. Slimane and T. Le-Ngoc. Tight bounds on the error probability of coded modulation schemes in Rayleigh-fading channels. *IEEE Trans. Vehic. Technol.*, 44(1):121–130, Feb. 1995.

[103] C.-E. W. Sundberg and N. Seshadri. Coded modulation for fading channels: An overview. *Eur. Trans. Telecommun. Rel. Technol.*, 4(3):309–324, May 1993.

[104] C. Tellambura, Q. Wang, and V. K. Bhargava. A performance analysis of trellis-coded modulation schemes over Rician-fading channels. *IEEE Trans. Vehic. Technol.*, 42(4):491–501, Nov. 1993.

[105] C. Tellambura, Q. Wang, and V. K. Bhargava. Performance of trellis-coded modulation schemes on shadowed mobile satellite communication channels. *IEEE Trans. Vehic. Technol.*, 43(1):128–139, Feb. 1994.

[106] P. J. Tourtier, R. Monnier, and P. Lopez. Multicarrier modem for digital HDTV terrestrial broadcasting. *Signal Proc.: Image Commun.*, 5(5–6):379–403, Dec. 1993.

[107] J. C. Tu. *Theory, design and application of multi-channel modulation for digital communications.* PhD thesis, Stanford University, CA, June 1991.

[108] A. Vahlin and N. Holte. Optimal finite duration pulses for OFDM. *IEEE Trans. Commun.*, 44(1):10–14, Jan. 1996.

[109] M. Vetterli and J. Kovacevic. *Wavelets and subband coding.* Prentice Hall, Englewood Cliffs, N.J., 1995.

[110] E. Viterbo and K. Fazel. How to combat long echoes in OFDM transmission schemes: Sub-channel equalization or more powerful channel coding. In *Proc. Globecom*, volume 3, pages 2069–2074, Singapore, Nov. 1995.

[111] B. Vucetic and J. Du. The effects of phase noise on trellis-coded modulation over Gaussian and fading channels. *IEEE Trans. Commun.*, 43(2/3/4):252–260, 1995.

[112] M. Wahlqvist, R. Larsson, and C. Östberg. Time synchronization in the uplink of an OFDM system. In *Proc. IEEE Vehic. Technol. Conf.*, volume 3, pages 1569–1573, Atlanta, GA, Apr. 1996.

[113] M. Wahlqvist, C. Östberg, J.-J. van de Beek, O. Edfors, and P. O. Börjesson. A conceptual study of OFDM-based multiple access schemes: Part 1 – Air interface requirements. Technical Report Tdoc 116/96, ETSI STC SMG2 meeting no 18, Helsinki, Finland, May 1996.

[114] W. D. Warner and C. Leung. OFDM/FM frame synchronization for mobile radio data communication. *IEEE Trans. Vehic. Technol.*, 42(3):302–313, Aug. 1993.

[115] L. Wei and C. Schlegel. Synchronization requirements for multi-user OFDM on satellite mobile and two-path Rayleigh-fading channels. *IEEE Trans. Commun.*, 43(2/3/4):887–895, Feb/Mar/Apr 1995.

[116] S. B. Weinstein and P. M. Ebert. Data transmission by frequency-division multiplexing using the discrete Fourier transform. *IEEE Trans. Commun.*, COM-19(5):628–634, Oct. 1971.

[117] J.-J. Werner. The HDSL environment. *IEEE J. Select. Areas Commun.*, SAC-9(6):785–800, Aug. 1991.

[118] S. K. Wilson. *Digital audio broadcasting in a fading and dispersive channel*. PhD thesis, Stanford University, CA, Aug. 1994.

[119] S. K. Wilson, R. E. Khayata, and J. M. Cioffi. 16-QAM modulation with orthogonal frequency-division multiplexing in a Rayleigh-fading environment. In *Proc. IEEE Vehic. Technol. Conf.*, volume 3, pages 1660–1664, Stockholm, Sweden, June 1994.

[120] Y. Wu and B. Caron. Digital television terrestrial broadcasting. *IEEE Commun. Mag.*, 32(5):46–52, May 1994.

[121] G. Young, K. T. Foster, and J. W. Cook. Broadband multimedia delivery over copper. *BT Technol. Journ.*, 13(4):78–96, Oct. 1995.

[122] E. Zehavi and J. K. Wolf. On the performance evaluation of trellis codes. *IEEE Trans Inform. Theory*, IT-33(2):196–202, Mar. 1987.

[123] T. N. Zogakis, J. T. J. Aslanis, and J. M. Cioffi. Analysis of a concatenated coding scheme for a discrete multitone modulation system. In *Proc. IEEE Military Commun. Conf.*, volume 2, pages 433–437, Long Branch, NJ, Oct. 1994.

[124] T. N. Zogakis, P. S. Chow, J. T. Aslanis, and J. M. Cioffi. Impulse noise mitigation strategies for multicarrier modulation. In *Proc. Intern. Conf. Commun.*, pages 784–788, Geneva, May 1993.

[125] T. N. Zogakis and J. M. Cioffi. The effects of timing jitter on the performance of a discrete multitone system. *IEEE Trans. Commun.*, 44(7):799–808, July 1996.

[126] W. Y. Zou and Y. Wu. COFDM: An overview. *IEEE Trans. Broadc.*, 41(1):1–8, Mar. 1995.

# Index